SLAC-PUB-1213
COO-2220-10
(T)
March 1973

CORRESPONDENCE ARGUMENTS FOR HIGH ENERGY COLLISIONS

J. D. Bjorken*

Stanford Linear Accelerator Center
Stanford University, Stanford, California 94305

and

J. Kogut†

Institute for Advanced Study
Princeton University, Princeton, New Jersey 08540

(Submitted to Phys. Rev.)

---

*Work supported by the U. S. Atomic Energy Commission.

†Work supported by the U. S. Atomic Energy Commission, Contract No. AT(11-1)-2220.

ABSTRACT

We assume that in deep-inelastic processes such as $e^- p \to e^- +$ hadrons, $\nu_\mu p \to \mu^- +$ hadrons, $e^+ e^- \to$ hadrons, or $pp \to$ hadrons of high transverse momentum, the dynamics is continuously and smoothly connected to their limiting cases. For example, the process $\gamma p \to$ hadrons is a limit of $e^- p \to e^- +$ hadrons, exclusive channels are limiting cases of inclusive spectra, and $pp \to$ low-p_T hadrons is a limiting case of $pp \to$ high-p_T hadrons. The demand that these limits be smooth we call correspondence (with apologies to Bohr). Correspondence evidently is closely related to the concept of duality, although much cruder, at least in the way we practice it. We first apply the correspondence method to some familiar examples. However, the main applications are to the processes $e^- p \to e^- +$ hadrons, $\nu p \to \mu +$ hadrons, and $e^+ e^- \to$ hadrons. We find find several properties of hadron inclusive distributions and exclusive channels to be roughly independent of Q^2, in particular (a) the scaled inclusive momentum distribution in colliding beam processes, (b) hadron inclusive distributions (and therefore multiplicity) at a given s in electroproduction, (c) the ratio of nondiffractive exclusive electroproduction cross sections (such as $e^- p \to e^- \pi^+ n$) to total electroproduction cross sections at fixed s, and (d) the ratio of the cross section for coherent electroproduction of all vector states to the total electroproduction cross section. Some semi-quantitative estimates are given.

TABLE OF CONTENTS

I. Introduction

II. Hadron-Hadron Collisions

A. Main Features of Pure Hadronic Reactions

B. Inclusive-Exclusive Connections

C. Applications to Hadron-Hadron Reactions at Fixed Angles

D. A Caveat: Diffraction-Dissociation

III. Deep Inelastic Electroproduction and e^+e^- Annihilation

A. Use of Correspondence to Estimate $\sigma_T + \sigma_S$

B. e^+e^- Annihilation into Hadrons

C. Hadron Inclusive Spectrum in Deep-Inelastic Electroproduction

D. Inclusive-Exclusive Connections in Electroproduction

E. Properties of Exclusive Channels in Electroproduction

F. Connection of Photon Fragmentation with Vector Dominance

G. Coherent Production of Vector States

H. The Central Plateau in the Photon Fragmentation Region

IV. Semiquantitative Estimates of Cross Sections

A. $pp \rightarrow \pi^o$ + Hadrons

B. $pp \rightarrow p$ + Hadrons

C. Hadron Distribution in e^+e^- Annihilation

D. Exclusive Electroproduction of a π^+

V. Summary and Conclusions

I. INTRODUCTION

With the advent of new accelerators and the inevitable data explosion accompanying them we may expect a continuing expansion of the frontiers of hadron physics, including the "deep inelastic" physics associated with lepton-hadron interactions. Many of those frontiers are relatively new ones — for example, the high p_T region in hadron-hadron collisions, the production of high energy hadrons in e^+e^- collisions, and the detailed study of the hadrons produced in deep-inelastic e^-p, μp, and νp collisions. It is always tempting, and it may even be correct, to anticipate completely new dynamical mechanisms to be operating in these regions. However, it is our purpose here to lean as far as possible the other way, and suppose that the dynamics in the new kinematic regimes (e.g., high p_T in hadron-hadron collisions, high energy in e^+e^- annihilation, high Q^2 in the deep inelastic lepton-induced processes) is very closely and continuously linked with the dynamics in the old regime (defined by replacing "high" by "low" between the previous parentheses). This hypothesis, to be considered a working hypothesis, is made for more than reasons of taste. There is already more than one piece of evidence that this kind of continuity works. Duality is a perfect example: A Regge-pole description designed for high energy works, on the average, all the way through the resonance region for π-N scattering.[1] A related and beautiful example[2] is the dip-structure of two-body scattering amplitudes, which appears at high energy to occur at a fixed value of t, independent of s. Furthermore, the positions of the dips are related to zeros of the Bessel-functions $J_i(b\sqrt{-t})$ which appear in an impact-parameter description of the process. When s is extended into the resonance region, the dips, even at resonances, persist, where they are related to zeros of the Legendre function describing the angular distribution at the resonance.

Thus, a connection between spin and energy of the resonances can be established, just from knowledge of the high-energy phenomenon and the assumed continuity in the dynamics.

But, in addition to relating two known regions, the demand of continuity of dynamical description allows one to sometimes infer properties of the dynamics in new kinematical regimes in terms of known or almost known behavior on the boundary of that regime or in old kinematical regimes. In all these cases there is a similarity to Bohr's use of the correspondence principle[3] in connecting the behavior of a quantum theory with the (known) classical limit, thereby gaining information on the nature of the quantum theory itself. In our examples there will be an "unknown" kinematical region, about which we wish to learn something, and a neighboring "known" one about which we already hold some information. "Correspondence", i.e., continuity in the dynamics provides the link. In addition, some hypothesis or limited information about the unknown region is usually necessary to obtain some useful result.

This article is organized as follows. Section II is devoted to simple examples of the correspondence method in a hopefully familiar context. We first review briefly the gross features of inclusive hadronic reactions and the assumption of short range correlations in rapidity. Then two correspondence arguments connecting inclusive and exclusive processes are discussed. The first applies to hadron reactions at fixed p_T and gives the familiar Feynman boundary condition,[4] while the second applies to processes at fixed angle and approximates work done by Gunion, Brodsky, and Blankenbecler.[5,6] An interpolation formula for inclusive reactions at low and high p_T is presented. Then diffraction dissociation is briefly discussed as an apparent exception to the use of correspondence to get an inclusive-exclusive connection. Section III contains the

main results of the paper. It concerns less familiar aspects of deep inelastic electroproduction and e^+e^- annihilation processes. As a prelude, correspondence is used to motivate the scaling phenomenon and the shape of νW_2. Then gross features of the total annihilation cross section and inclusive spectra are obtained via correspondence and the assumption of short range correlations in rapidity. The hadron spectrum in deep inelastic electroproduction is discussed and inclusive-exclusive connections are made. Interesting information on form factors and structure functions emerge. Individual electroproduction channels are discussed and the high and low ω dependence of forward and backward production of pions is roughly determined. The photon fragmentation region is discussed from a vector meson dominance point of view. The "aligned-jet" version of generalized vector dominance[7] is reviewed and the hadron spectrum in the photon fragmentation region is related to that in e^+e^- annihilation. The idea of hole fragmentation[8] emerges naturally. Coherent production of vector states is considered. Finally, the height of the plateau in the photon fragmentation region is related to the height of the central region. In Section IV semi-quantitative estimates are made and curves are presented for several of the reactions discussed in the text. These include fixed angle proton and pion distributions in proton-proton collisions, inclusive pion and proton production in e^+e^- annihilation, and forward and backward electroproduction of pions. Many of these results can be expressed as the Q^2 independence of certain distribution functions or ratios of cross sections under appropriate kinematic conditions. Finally, Section V contains some concluding words.

II. HADRON-HADRON COLLISIONS

A. Main Features of Pure Hadronic Reactions

In several of our examples of correspondence it is necessary to make some dynamical assumptions about the production mechanism in inclusive hadronic processes $A+B \to C+\text{anything}$. We shall make the popular assumption of short range correlation in rapidity,[9,10] which we review below. One could instead adopt a diffraction-excitation (fireball, nova) picture[10] of multiparticle production and develop correspondence arguments for them. For us, however, the short range correlation assumption seems to lead more easily to a satisfactory and consistent overall dynamical scheme. But that may be a consequence of personal prejudice and it should be possible to produce an equally credible scheme based on diffraction excitation (or even connect them smoothly by considering the dependence of the dynamics on impact-parameter (see Section II. D). Some applications of the diffraction-excitation model will be considered from time to time in the text.

To begin, recall some of the general features of hadronic reactions $A+B \to C+\text{anything}$. Let A denote the projectile and B the target and call the beam direction the z axis (the component of a momentum vector along the z axis will be written p_z or, alternatively, $p_\parallel$). The differential cross section for observing C can be written in the invariant, dimensionless form,

$$\frac{1}{\sigma} E_c \frac{d^3\sigma}{dp_c^3} = F_{AB \to C}(x, p_T^2; s) \qquad \text{(II. 1)}$$

where $x = p_\parallel^c / p_\parallel^{max}$, $s = E_{cm}^2$, and p_T is the momentum of C transverse to the beam direction. In the limit of large s the function F tends toward a nonvanishing

function of the dimensionless variable x and p_T^2,

$$F(x, p_T^2; s) \xrightarrow[s \text{ large}]{} F(x, p_T^2) \tag{II. 2}$$

Furthermore, the transverse momentum distributions of secondaries in hadronic inclusive reactions fall off rapidly with p_T (e.g., as p_T^{-n} with n large, or $\exp(-ap_T)$, etc.).

In light of the rapid falloff of $F(x, p_T^2)$ with increasing p_T, it is sensible to consider the distribution of secondaries as a function of x ($-1 \leq x \leq +1$). Equivalently, one can plot the number distribution against the related variable rapidity,

$$y = \frac{1}{2} \log\left(\frac{E + p_z}{E - p_z}\right) \tag{II. 3}$$

which varies from $-\frac{1}{2}\ell n\, s$ to $+\frac{1}{2}\ell n\, s$. In terms of rapidity, the distribution function F expected theoretically and observed experimentally is depicted schematically in Fig. 1. The rapidity of target B is marked on the left of the rapidity axis and that of the projectile A on its right. If the rapidity of particle C lies within a few units of the target B, its distribution function will depend on the character of B. This region is called the target fragmentation region. Similarly, the region within a few units of the right-hand end of the rapidity plot is denoted the projectile fragmentation region. However, choosing C to lie far from the boundaries A and B, the assumption of short range correlation in rapidity implies that the distribution function of C becomes independent of both target and projectile. Since a longitudinal Lorentz boost is just a translation in y, the rapidity plot should become flat and universal (independent of A and B) in this region.

This central region or central "plateau" has a length on the rapidity axis which is $\sim \ell n\ s$. The height c of the inclusive distribution function dN/dy is clearly related to the mean multiplicity $\bar{n}$ of hadrons in $A+B \to$ anything via $\bar{n} = c \ell n\ s + \text{const.}$

B. Inclusive-Exclusive Connections

The first example of correspondence connects properties of such inclusive particle spectra with two-body exclusive scattering processes. For this first part of the argument we need not assume any of the general picture of short-range correlations described in the previous section. Consider the momentum spectrum of particle C in the process $A+B \to C+$anything, at either fixed angle or fixed p_T. For definiteness consider the reaction in the center-of-mass frame. As the momentum p of particle C increases, the missing mass of the unobserved system "anything" (call it D) decreases, until one reaches the "resonance" region where the mass m_D of the missing system is $\lesssim$ some fixed amount, say 2 GeV. (By dubbing this region the resonance region, we do not mean to imply that there are no resonances outside it, but only that resonances prominent in inclusive experiments are contained within it.) We now look at $E\,(d^3\sigma/dp^3)$ vs p, illustrated schematically in Fig. 2.

Now suppose we have a formula (such as (II. 2)) for the inclusive distribution function F which provides a smooth extrapolation into the resonance region. The correspondence argument in this case states that the resonance contribution should be comparable in magnitude to the extrapolated continuum. Why? If the continuum can be regarded as built of resonances (e.g., dual resonance models), it is evidently so; that is the definition of the continuum. But another viewpoint leading to the same conclusion is that the matrix elements responsible for the inclusive process may be smoothly extended into the resonance region with the

only modification being (1) breaking them up into contributions of a small number of partial waves for the system D (because M_D is bounded) and (2) enhancing the resonant partial waves by Breit-Wigner final-state interaction factors. Thus, a finite fraction of the inclusive cross section has been enhanced by a finite factor, leading again to the conclusion that the resonance contributions are of the same order of magnitude as the extrapolated inclusive contribution in the resonance region. This is formalized in the expression,

$$\int_{p_{max} - \frac{m_D^2}{4p_{max}}}^{p_{max}} E\frac{d^3\sigma}{dp^3}\Big|_{inclusive} dp \sim \sum_{resonances} E\frac{d\sigma}{dp_T^2}\Big|_{exclusive} \qquad (II.4)$$

where the integration region over the inclusive spectrum,

$$p \gtrsim p_{max} - \frac{m_D^2}{4p_{max}} \qquad (II.5)$$

ensures that the missing mass is at most the finite quantity m_D. Equation (II.4) does not mean exact equality. Instead it states that there should be no systematic variation of the ratio of the right- and left-hand sides with external parameters such as beam energy, p_T and θ. In other words, from the point of view of "missing mass" experiments, the signal/noise ratio is always 0(1). As an example of how (II.4) may be used, we may take the limiting fragmentation hypothesis for the behavior of the inclusive distribution and Regge behavior for the exclusive cross sections. For $p \approx p_{max}$,

$$E\frac{d^3\sigma}{dp^3} \sim f(p_T^2)\left(1 - \frac{p}{p_{max}}\right)^n \qquad (II.6)$$

and for the exclusive channel,

$$\frac{d^2\sigma}{dp_T^2} \sim g(p_T^2)\,(p_{max}^2)^{2\alpha(p_T^2)-2} \qquad \text{(II. 7)}$$

where $\alpha(p_T^2)$ is the leading Regge-trajectory in the $A\bar{C}$ channel. Inserting (II. 6) and (II. 7) into (II. 4) implies,

$$p_{max}^{-2n-1} \sim p_{max}^{4\alpha-3} \qquad \text{or} \qquad n = 1-2\,\alpha(0) \qquad \text{(II. 8)}$$

Equation (II. 8), which relates the energy dependence of the exclusive channel and the shape of the high energy end of the inclusive cross section, was suggested by Feynman,[4] and follows also from Mueller's analysis.[11]

Another, albeit minor, relation follows from Eq. (II. 4) by matching the p_T dependences of the inclusive and exclusive channels. Suppose that the exclusive channel is dominated by a moving Regge pole: $\alpha(p_T^2) = \alpha_0 + \alpha' p_T^2$. Then the p_T distribution shrinks as s increases,

$$\langle p_T^2 \rangle = \frac{\int p_T^2 \frac{d\sigma}{dp_T^2}\, dp_T^2}{\int \frac{d\sigma}{dp_T^2}\, dp_T^2} = (\text{const.} + 2\alpha' \ell n\, s)^{-1} \qquad \text{(II. 9)}$$

But Eq. (II. 4) implies that the average transverse momentum of fast secondaries in the inclusive reaction should have the same weak s dependence.

The shrinkage of the p_T distribution in elastic processes has proved very difficult to verify or reject experimentally . Accordingly, shrinkage in the inclusive reaction represents a delicate effect and, aside from being difficult to study experimentally, may well be an overextension of the correspondence arguments, which are intended for relatively crude estimates.

C. Applications to Hadron-Hadron Reactions at Fixed Angles

Another less familiar example lies in relating fixed-angle behavior for hadron-hadron inclusive and exclusive processes. For example Blankenbecler, Brodsky and Gunion[5,6] propose a parton exchange model for elastic hadron-hadron scattering, which in fact generalizes the mechanism envisaged by Feynman[4] for ordinary collisions. Their result is that for large angles,

$$\left(\frac{d\sigma}{d\Omega}\right)_{cm} \sim \frac{1}{s^a (\sin\theta_{cm})^b} \qquad \text{(II. 10)}$$

where empirically (and theoretically!),

$$a \sim 10 \text{ to } 12 \qquad b \sim 12 \qquad \text{(II. 11)}$$

The parton-exchange mechanism at low p_T is supposed to lead to an inclusive distribution for the process $p+p \to p+$anything of the form,

$$E\frac{d^3\sigma}{dp^3} \sim f(p_T^2) \qquad \text{(II. 12)}$$

Since we suppose that the same parton-exchange mechanism is responsible for the physics at both boundaries of the Peyrou plot, it may be reasonable to invoke the correspondence argument and seek a smooth interpolating function to connect these extreme boundary regions. We choose, mainly for simplicity and the expectation that small missing mass m_D provides the dominant suppression mechanism near the boundary of phase space,

$$E\frac{d^3\sigma}{dp^3} \sim f(p_T^2)\left(1 - \frac{p}{p_{max}}\right)^n \qquad \text{(II. 13)}$$

and use again the inclusive-exclusive correspondence argument,

$$\int_{p_{max}-\frac{m_D^2}{4p_{max}}}^{p_{max}} \frac{d^2\sigma}{d\Omega dp}\, dp \sim p_{max}\, f(p_{max}^2 \sin^2\theta)\, \frac{1}{p_{max}^n} \left(\frac{const}{p_{max}}\right)^{n+1}$$

$$\sim \left(\frac{d\sigma}{d\Omega}\right)_{cm} \qquad \text{(II. 14)}$$

We conclude from (II. 9) and (II. 13) that,

$$f(p_T^2) \sim \frac{1}{p_T^b} \qquad \text{(II. 15)}$$

and,

$$n \sim a - b/2 \qquad \text{(II. 16)}$$

With the numbers given in Eq. (II. 10), this leads to the inclusive distribution of protons of high p_T in pp collisions to be,

$$E\,\frac{d^3\sigma}{dp^3} \sim \frac{1}{p_T^b} \left(1 - \frac{p}{p_{max}}\right)^{a-\frac{b}{2}} \sim \frac{1}{p_T^{12}} \left(1 - \frac{p}{p_{max}}\right)^{4 \text{ to } 6} \qquad \text{(II. 17)}$$

in agreement with a direct model calculation.

The pion yield in pp collisions is difficult to estimate directly because the $p \approx p_{max}$ boundary of phase space is controlled by exotic processes, e.g., $pp \rightarrow \pi^+ + d$. However, an indirect approach can be taken. Blankenbecler, Brodsky, and Gunion[5] predict wide angle pion-nucleon scattering,

$$\left(\frac{d\sigma}{d\Omega}\right)_{cm} \sim \frac{1}{s^{a_\pi}} \frac{1}{(\sin\theta_{cm})^{b_\pi}} \qquad \text{(II. 18)}$$

where

$$a_\pi \sim 7 \qquad b_\pi \sim 8 \qquad \text{(II. 19)}$$

The inclusive-exclusive argument connects these parameters to the inclusive spectrum $\pi p \to \pi +$ anything,

$$E \frac{d^3\sigma}{dp^3} \sim \frac{1}{p_T^8} \left(1 - \frac{p}{p_{max}}\right)^3 \qquad \text{(II. 20)}$$

To relate this spectrum to $pp \to \pi +$ anything recall that the distribution for the central region is universal and applies equally to $pp \to \pi + X$ and $\pi p \to \pi + X$. So, for $p \ll p_{max}$, we expect

$$E \frac{d^3\sigma}{dp^3} \sim \frac{1}{p_T^8} \qquad \text{(II. 21)}$$

for $pp \to \pi +$ anything.

D. A Caveat: Diffraction Dissociation

We now turn to an example where the inclusive-exclusive connection does not work: inclusive production of protons at small p_T in pp collisions. The inclusive distribution is shown schematically in Fig. 3. The smooth inclusive distribution is roughly constant in p; the inclusive-exclusive connection (II. 4) implies that $\alpha(0) \sim 1/2$ or $\frac{d\sigma}{dt}\Big|_{exclusive} \sim s^{-2}$. However, elastic scattering and diffraction dissociation processes $pp \to N^*(1536)$, $N^*(1688)$ (or $\pi N \to (A1)N$, $KN \to QN$) have roughly constant cross sections and are not connected smoothly to the inclusive continuum. This contradicts our simple correspondence arguments. We suspect the resolution of this contradiction lies in the dependence of the dynamics on the impact-parameter b. At the large impact-parameters important for elastic scattering or diffraction dissociation, absorptive effects are not important, while at small impact parameters absorption is nearly complete and multiparticle production dominates. The two regions of very small b and large b may be as different as black from white. It is a challenge for the

correspondence method to suggest even a rough interpolation of the inclusive processes from large to small b. We have not succeeded in doing this in the context of the hypothesis of short-range correlation. Such a connection, however, poses no difficulty for the diffraction-excitation picture where the dynamical mechanism is the same at all impact-parameters. It indeed provides a major intuitive motivation for that model.

III. DEEP INELASTIC ELECTROPRODUCTION AND e^+e^- ANNIHILATION

A. Use of Correspondence to Estimate $\sigma_T+\sigma_S$

As another example of correspondence arguments, we examine what inferences may be made about the form of the deep-inelastic structure function.[12] We choose to discuss the cross section $\sigma(Q^2,\nu) = \sigma_T+\sigma_S$ in the region of large Q^2 and ν. The Q^2-ν space, described in Fig. 4, has boundaries $Q^2=0$ (photoproduction) and $Q^2=2M\nu$ (elastic scattering). We assume the behavior of the photoproduction boundary $\sigma(Q^2,\nu) \to$ const as $\nu \to \infty$, and $\sigma_{el}(Q^2,\nu) \sim \delta(\nu - Q^2/2M)\, G^2(Q^2) \sim \delta(\nu - Q^2/2M)(Q^2)^{-2n}$ along the elastic-scattering line. For fixed missing mass, $s = 2M\nu - Q^2+M^2$ (see Fig. 4), we expect σ to behave similarly to the elastic form factor. For fixed Q^2 and $\nu \to \infty$, we anticipate $\sigma \to f(Q^2)$ by either using the correspondence argument or the argument that Regge trajectories should not depend upon Q^2.

We now use two additional clues to guess the behavior of σ. One is kinematical and the other is a sum rule. The kinematical argument is that the minimum momentum transfer for a t-channel exchange process becomes large when $\omega = 2M\nu/Q^2$ or $\omega' = 1+s/Q^2$ becomes small.[13] The minimum longitudinal momentum transfer $\Delta^2_{min} = -t_{min} = \frac{M^2}{\omega(\omega-1)} + \frac{M_f^2 - M^2}{\omega-1}$ scales as ω^{-1}. When Δ_{min} becomes large we must (by default) expect s-channel processes to be most important. For $\omega' \gg 3$, Δ_{min} is so small that coherent processes (such as $\gamma^*+p \to \rho+p$) have established themselves and we expect the asymptotic behavior $\sigma \sim f(Q^2)$ to have set in. Hence, a reasonable form for all ω' is

$$\sigma \sim h(\omega)\, f(Q^2) \sim \left(\frac{\omega'-1}{\omega'}\right)^p f(Q^2) \sim \left(\frac{\omega'-1}{\omega'}\right)^p (Q^2)^{-m} \qquad \text{(III. 1)}$$

where the power behaviors are motivated by the observed power-law behavior in $G(Q^2)$. From this much we get, using the inclusive-exclusive connection

described earlier,

$$\int_1^{1+\frac{\text{const}}{Q^2}} \sigma(Q^2,\nu)\, d\omega' \sim \int_{\text{Resonances}} \sigma_{el}\, d\omega' \qquad \text{(III. 2)}$$

or

$$(Q^2)^{-m-p} \sim (Q^2)^{-2n} \quad . \qquad \text{(III. 3)}$$

To go further requires use of current-algebra sum rules, in particular the inequality[14] derived from Adler's sum rule[15] for neutrino processes,

$$\int_0^{\nu_{max}(Q^2)} \sigma(Q^2,\nu)\, \frac{d\nu}{\nu} \gtrsim \frac{\text{const}}{Q^2} \qquad \text{(III. 4)}$$

where $\nu_{max}(Q^2)$ is expected (from the Δ_{min} arguments given previously) to be $\sim (\text{const})\, Q^2$. This leads to,

$$\int_1^{\text{const}} h(\omega)\, f(Q^2)\, \frac{d\omega}{\omega} \sim (Q^2)^{-1} \qquad \text{(III. 5)}$$

or

$$m=1$$

and consequently,

$$p=2n-1 \qquad \text{(III. 6)}$$

the relation given by Drell and Yan[16] and by Bloom and Gilman.[17]

Thus, just from correspondence and from some quite simple and general considerations, one obtains a good first-order understanding of the general shape and size of the deep-inelastic structure function. Of course, these relations are all somewhat loose, even the relations between the power-law indices, and they are meant as a first semiquantitative guide and a framework on which to build more precisely formulated ideas.

B. e^+e^- Annihilation into Hadrons

At high energy hadron production by e^+e^- colliding beams is dominated by the two-photon mechanism

$$e^+e^- \to e^+e^- + \text{hadrons} \qquad \text{(III. 7)}$$

the dynamics of which is closely related, via vector dominance, to $\rho^o+\rho^o \to$ hadrons. However, the one-photon process,

$$e^+e^- \to \text{hadrons} \qquad \text{(III. 8)}$$

is a most uncommon one, about which we have little insight. It is popular to expect,[18] by analogy with the scaling behavior of deep-inelastic electroproduction, that the total cross section for the one-photon process is scale invariant

$$\sigma_{tot} \sim (Q^2)^{-1} \qquad \text{(III. 9)}$$

where Q is the total c.m.s. energy of the e^+e^- pair. Furthermore experiments[19] indicate $\sigma_{tot}/\sigma(e^+e^- \to \mu^+\mu^-) > 1$, supporting this conjecture of large cross section at high Q^2. We shall for definiteness assume (III. 9) here. Also, as an additional boundary condition it is expected that the electromagnetic form factor of any hadron will fall with increasing timelike Q^2 as a power: $G_i(Q^2) \sim (Q^2)^{-n_i}$ with $n \sim 2$ for the nucleon. This in itself implies, given the inclusive-exclusive connection, that the inclusive momentum distribution of hadrons falls as a power, not an exponential of the momentum. We now develop this connection in more detail.

The most general inclusive distribution for unpolarized e^+ and e^- to produce hadron i of momentum p and angle θ is,

$$p\frac{d^2\sigma}{d\Omega dp} = A(p) + B(p)\cos^2\theta \quad . \qquad \text{(III. 10)}$$

We shall not have any special concern for the angular dependence, and immediately take an angular average, writing,

$$\frac{1}{\sigma_{tot}} p \frac{d\sigma_i}{dp} = f_i(p, Q) \tag{III. 11}$$

Near the endpoint $p \sim p_{max}$ we expect a power-law approach, and write,

$$f_i(p, Q) \sim \left(1 - \frac{p}{p_{max}}\right)^{p_i} \frac{1}{Q^{m_i}} \tag{III. 12}$$

The behavior of $f_i(p, Q)$ is then related to the elastic cross section,

$$\sigma_{el} \sim \frac{1}{Q^2} G^2(Q^2) \sim \frac{1}{(Q^2)^{1+2n_i}} \tag{III. 13}$$

By the correspondence hypothesis,

$$\int_{Q-\frac{const}{Q}}^{Q} \frac{d\sigma}{dp} dp \sim \frac{1}{Q^3} \frac{1}{Q^{m+p_i}} \left(\frac{const}{Q}\right)^{p_i+1} \sim \sigma_{el} \tag{III. 14}$$

yielding,

$$4 + m_i + 2p_i = 2 + 4n_i \tag{III. 15}$$

Parton models[20] or, more generally, a scaling hypothesis for the inclusive distribution function suggest $m_i=0$, in which case we obtain again the Drell-Yan[16] threshold theorem,

$$p_i = 2n_i - 1 \tag{III. 16}$$

in this case for timelike Q^2. If,

$$f_i(p, Q) = f_i(p/Q) \tag{III. 17}$$

and $f_i(0) \rightarrow$ const, we obtain a logarithmic increase in multiplicity with Q^2, a behavior very compatible with that found in hadron physics.

Various models have from time-to-time[21] predicted $\bar{n} < \infty$ as $Q^2 \to \infty$. This behavior violates our correspondence ideas. If $\sigma_{tot} \sim 1/Q^2$ and $\bar{n}$ is finite, then there must exist some exclusive cross section σ_m which scales, i.e., $\sigma_m \sim 1/Q^2$. However, according to the correspondence idea, the asymptotic behavior of σ_m in Q^2 should not differ significantly from $\sigma(e^+e^- \to \pi^+\pi^-)$ or $\sigma(e^+e^- \to p\bar{p})$ which certainly do not scale. Thus, we have our choice of $\bar{n} \sim \log Q^2$, and $f_i(0) \sim$ const or $\bar{n} \sim (Q^2)^\delta$ which is a hypothesis more in line with ideas of "pulverization,"[22] nova production,[10] or statistical production.[23] There one might assume that,

$$\frac{1}{\sigma_{tot}} p \frac{d\sigma_i}{dp} \sim \left(\frac{\mu_0^2}{p^2 + \mu_0^2} \right)^{\frac{m_i}{2}} \qquad \text{(III. 18)}$$

i.e., the scale of p is absolute rather than relative to Q. In this case the mean multiplicity $\bar{n} \sim \sqrt{Q^2}$, provided $m > 0$. If the form (III. 18) is used to the boundary of phase space (this means $p_i = 0$ in Eq. (III. 12)), we get from the inclusive-exclusive connection

$$m_i = 4n_i - 2 \qquad \text{(III. 19)}$$

or, with the more general case (III. 12),

$$0 < m_i < 4n_i - 2 \qquad \text{(III. 20)}$$

It is tempting to suppose that these "fireballs" would be closely related to the novas or fireballs occurring in diffraction-excitation models. This would again lead to a power-law decrease of p_T distributions with (for large $\theta_{c.m.}$),

$$\frac{d\sigma_i}{dp_T^2} \sim \frac{\text{const}}{p_T^{m_i+2}} \qquad \left(p_T^2 \ll s\right) \qquad \text{(III. 21)}$$

in ordinary hadron-hadron collisions. With $n_i \leq 2$ for i=N or π, this gives

$$\frac{d\sigma}{dp_T^2} \gtrsim \frac{\text{const}}{p_T^6} \qquad \text{(III. 22)}$$

which is a broad distribution indeed. But we may have entered into much too high a degree of speculation here in trying to connect e^+e^- annihilation with hadron-hadron collisions.

We have seen that the first hypothesis, in which the inclusive distribution scales, leads to a hadron distribution in $|p|$, and a mean multiplicity very similar to those in ordinary collisions. We may question whether the angular correlations are similar. That is, the produced particles in an ordinary hadron collision are approximately collinear, with $\langle p_T \rangle$ relative to the incident beams limited to $\sim$350 MeV. Because the intermediate single-γ state has J=1, there can be little memory of the e^+e^- collision axis. One has a choice between two extremes: one is that the reaction is "explosive": he final hadrons in a given event are distributed more or less randomly in phase-space. The other extreme is less unfamiliar: the "collision axis" of a given event is determined by the direction of the leading particle (the hadron with the highest p, $p \sim$ (const) Q), and the $\langle p_T \rangle$ of all other produced hadrons is small ($\sim$350 MeV) relative to this axis. Such a configuration tends to maximize the number of low subenergies of pairs of produced hadrons. Hereafter we shall adopt this configuration as well as the scaled inclusive distribution in going on to study electroproduction and neutrino production of hadrons.

C. Hadron Inclusive Spectra in Deep-Inelastic Electroproduction

Now we will attempt to apply these ideas to electroproduction. In particular, consider the inclusive process $\gamma^* + B \rightarrow C + \text{anything}$ for large Q^2 and s. Suppose also that at fixed, large Q^2, the final state hadron distribution still possesses

only short range correlations. Using the correspondence ideas we can estimate the sizes of the photon fragmentation region, the central region and the target fragmentation region for various values of Q^2. For $Q^2=0$ (photoproduction) one expects (on the basis of vector meson dominance, say) and finds experimentally that the inclusive spectrum is similar to that of hadron induced inclusive spectra.[24] The photon fragmentation region, for example, at $Q^2=0$ should be characteristic of pure hadronic reactions and have a length of about 2 units of rapidity. The spectrum of secondaries is expected, therefore, to be well represented by Fig. 1. Now let the photon become virtual and suppose that s is very large, $s >> Q^2$. Then the size of the projectile fragmentation region may change and the character of the inclusive distribution could change there. However, the assumption of short range correlations implies that the target fragmentation region remains unchanged in size and character.[25] Therefore, the remaining interval of rapidity $\sim(\ell n\ s - 2)$ is divided between the central and photon fragmentation regions. To estimate the length of the photon fragmentation region suppose that we start at fixed, large Q^2 and choose s very large. Now let s decrease until the projectile and target fragmentation regions merge. This occurs by the time that $\omega' = 1 + s/Q^2$ becomes a fixed, not too large number, 3 or 4, say. Two reasons can be cited for this: (1) For $\omega' \lesssim 3-4$, the proton structure function is considerably different from the neutron structure function. Certainly dominance of Pomeron exchange is a necessary condition for the existence of a central plateau. (2) The minimum momentum transferred between the virtual photon and the target is no longer small at small ω'.[13] At $\omega'=4$ the length of the photon fragmentation region is, roughly, $\ell n\ s = \ell n\ s/Q^2 + \ell n\ Q^2 \approx \ell n\ Q^2$. So, in general, the photon fragmentation region grows as $\ell n\ Q^2$. Finally, since the available length of rapidity grows as $\ell n\ s$, the length of the central region

must grow as $\ell n\ s - \ell n\ Q^2 \approx \ell n\ \omega'$, for large ω'. So, for large Q^2, s and ω' the rapidity axis should be subdivided into the regions shown in Fig. 5. These general remarks are realized in the parton model, most multiperipheral models and follow as well from a Mueller analysis.[25]

The character of the single particle distribution function in the central region will be expected to be the same as that in typical hadron-hadron collisions because that region is insensitive to the change with Q^2 of the properties of the γ^*. In particular, the density of secondaries in this region should be characteristic of typical hadron-hadron collisions.

However, if ω' is small the target and projectile regions overlap and are not distinct. This means that, although s is large, the properties of the hadrons carrying a finite fraction of the momentum of the photon are expected to be strongly dependent, in general, on the properties of the target. Only when $\ell n\ \omega'$ becomes large enough that a substantial central region exists will the fragmentation regions become well-defined and distinct. Then the principle of short range correlations implies that the fragmentation regions become independent.

D. Inclusive-Exclusive Connections in Electroproduction

Consider single hadron inclusive electroproduction $\gamma^* + B \to C + \text{anything}$. The single hadron inclusive differential cross section reads,

$$\frac{1}{\sigma_{tot}} E_C \frac{d^3\sigma}{dp_C^3} = F_{\gamma B \to C}\left(x, p_T^2; s, Q^2\right) \qquad \text{(III. 23)}$$

where x is the usual Feynman scaling variable $x = p_{\parallel}^C / p_{\parallel}^{max}$, and p_T is measured transverse to the virtual photon momentum. In the case of photoproduction ($Q^2=0$), the conjecture that F becomes a nontrivial function of only x and p_T^2 in the limit $s \to \infty$ has considerable experimental support. Similarly, we now use correspondence and assume that for nonvanishing Q^2 the single hadron inclusive

cross section again becomes a function of the dimensionless variable x, p_T^2, and Q^2,

$$\frac{1}{\sigma_{tot}} E_C \frac{d^3\sigma}{dp_C^3} \xrightarrow[s\to\infty]{} F\left(x, p_T^2; Q^2\right) \qquad \text{(III. 24)}$$

This equation will play an essential role in what follows.

The use of correspondence now generates constraints between the inclusive spectrum (III. 24) and the exclusive channels which lie on its boundary. So, consider exclusive electroproduction reactions $\gamma^*+B \to C+D$. If ω' is very high, we expect that this reaction is Regge-behaved and that its cross section reads,

$$\sigma_{excl} \sim \frac{1}{Q^2} \omega^{2\alpha-2} F_{\alpha C}^2(Q^2) \qquad \text{(III. 25)}$$

where $F_{\alpha C}$ is the transition form factor between the exchanged Reggeon and particle C (Fig. 6). Equation (III. 25) is motivated by a simple multiperipheral model and the following heuristic argument. Imagine turning the strong interactions off so that Fig. 6 reduces to an elementary exchange graph. This point-like graph scales so,

$$\sigma_{excl} \sim \frac{1}{Q^2} f(\omega) \qquad \text{(III. 26)}$$

Now turn the strong interactions back on. The virtual photon vertex acquires a form factor, so (III. 26) becomes,

$$\sigma_{excl} \sim \frac{1}{Q^2} f_\alpha(\omega) F_{\alpha C}^2(Q^2) \qquad \text{(III. 27)}$$

Choosing $s >> Q^2$ one expects (III. 27) to become Regge-behaved. This requirement implies that $f_\alpha(\omega) \sim \omega^{2\alpha-2}$ for large ω in agreement with (III. 25).

Correspondence provides the link between the inclusive and exclusive reactions,

$$\int_{p_{max}-\frac{M_p^2}{4p_{max}}}^{p_{max}} E\frac{d^2\sigma}{dp_\parallel dp_T^2}\,dp_\parallel \sim \sum_{\text{Resonances}} \frac{d\sigma}{dp_T^2} \qquad \text{(III. 28)}$$

in the γ^*-B center-of-mass frame. By matching the x and p_T dependences in (III. 28) one recovers (1) the Feynman boundary condition for $\gamma^* + B \to C + \text{anything}$, and (2) the approximate equality of transverse momentum distributions of fast ($x \approx 1$) secondaries in the inclusive and exclusive reactions. These derivations are analogous to those considered in Section II.B for pure hadronic processes. New relations follow from (III. 28), however, by matching the Q^2 dependences. The inclusive cross section should scale, i.e., behave as Q^{-2}. The Q^2 dependence of the exclusive channel can be read off from (III. 25), so (III. 28) implies,

$$\frac{1}{Q^2} \sim \frac{1}{Q^2}\,(Q^2)^{2-2\alpha}\,F_{\alpha C}^2(Q^2) \qquad \text{(III. 29)}$$

Therefore, the large Q^2 behavior of the form factor is related to the intercept of the dominant exchange in the exclusive electroproduction channel,

$$F_{\alpha C}(Q^2) \sim (Q^2)^{\alpha-1} \qquad \text{(III. 30)}$$

For example, let the exchanged particle be a pion so α=0 and $F_{\alpha C}$ is the pion elastic form factor. Then,

$$F_\pi(Q^2) \sim \frac{1}{Q^2} \qquad \text{(III. 31)}$$

which seems quite reasonable and has some preliminary experimental support.[26] Furthermore, consider backward nucleon electroproduction. The proton Regge

intercept is approximately -1/2, so the proton's form factor is predicted to be,[27]

$$F_p(Q^2) \sim \frac{1}{(Q^2)^{1.5}} \qquad \text{(III. 32)}$$

Present fits to the proton form factor suggest $(Q^2)^{-1.7}$ for Q^2 up to ~ 9 GeV^2 and $(Q^2)^{-2.0}$ for Q^2 between 9 and 20 GeV^2. So, as far as simple power-behaved form factors are concerned, (III. 32) is not too bad.

It is not clear, however, how seriously one should interpret (III. 30). Perhaps the most sensible point of view is to say that the inclusive-exclusive connections favor meson form factors to fall more slowly with Q^2 than baryon form factors, and that there is a connection between the Regge intercepts of their trajectories and the power index. And it is reassuring that the predicted power dependences themselves are at least realistic.

Using the Bloom-Gilman[17] relation as discussed in Section III.A, one can take (III. 30) and relate α to the threshold behavior of νW_2,

$$\nu W_2^{(C)} \sim (\omega'-1)^{1-2\alpha_C} \qquad \text{(III. 33)}$$

Meson structure functions are, therefore, predicted to vanish more slowly near $\omega' \approx 1$ than baryon structure functions.

Plausible arguments have been given relating the high ω' region of νW_2 to Regge intercepts.[28] Equations (III. 30) and (III. 33) go further and relate the small ω' behavior of νW_2 to Regge intercepts. So, if one accepts (III. 33), then the dynamics controlling the shape of the structure function in the threshold and the Regge regions must be intimately related. We do not understand why this should be so.

Another argument can be made giving (III. 30) without assuming the specific Q^2 dependence of the differential cross section (III. 25) for the exclusive channel.

To do this we assume that the inclusive hadron distribution function for $e^+e^- \to C+\text{anything}$ has the same dependence on $x = p_C/p_C^{max}$ that the inclusive hadron distribution in $e+B \to e+C+\text{anything}$ has when ω' is very large.[29] As discussed in Section III.B, the Bloom-Gilman relation in the annihilation channel implies that if the inclusive spectrum for $e^+e^- \to C+\text{anything}$ behaves as $(1-x)^p$ near x=1, then $F_C(Q^2) \sim (Q^2)^{-(p+1)/2}$. But the dependence of the inclusive hadron distribution function for $\gamma^*+B \to C+\text{anything}$ upon the longitudinal fraction of C is given by (II.7),

$$\frac{1}{\sigma_{tot}} \frac{d\sigma_C}{dx} \sim (1-x)^{1-2\alpha} \qquad \text{(III.34)}$$

So, demanding that $p=1-2\alpha$ implies that $F_C(Q^2) \sim (Q^2)^{\alpha-1}$ as before.

E. Properties of Exclusive Channels in Electroproduction

Correspondence also allows us to relate the high and low ω behavior of individual exclusive electroproduction channels. We begin with Eq. (III.27)

$$\sigma_{excl}(\omega, Q^2) = \frac{1}{Q^2} f(\omega)\, F_C^2(Q^2)$$

which describes $\gamma^*+B \to C+D$. This equation will be assumed to hold for all values of ω (for ω large, $f(\omega) \sim \omega^{2\alpha-2}$). In addition to the arguments we have presented for the factored character of (III.27), there exist arguments based on the dual resonance model[30] and the light-cone formalism.[31] In addition there is the kinematical argument that minimum momentum-transfer Δ_{min} is the dominant variable in the region of small ω. That is, all the arguments of Section III.A (except the current algebra sum rule) can be mustered for the exclusive process as well.

Suppose first that hadron B is a proton and hadron C is a pion. As ω tends toward 1 it is sensible to assume that $f(\omega)$ is well approximated by a power of

$(\omega-1)$,

$$f(\omega) \sim (\omega-1)^{\gamma} \qquad \text{(III. 35)}$$

Now consider $\gamma^* + B \rightarrow$ anything near $\omega=1$. Since νW_2 behaves as $(\omega'-1)^{1-2\alpha_B}$ near threshold, the total $\gamma^* + B \rightarrow$ anything cross section must be,

$$\sigma_{tot} \sim \frac{1}{Q^2} (\omega-1)^{1-2\alpha_B} \qquad \text{(III. 36)}$$

However, near threshold only the exclusive channels are kinematically accessible. Therefore, if one integrates σ_{tot} over the resonance region $\left(\omega' \lesssim 1 + \frac{M_D^2}{Q^2}\right)$ one should obtain the same answer (order of magnitude) as the integral over the two-body exclusive channels:

$$\int_1^{1+\frac{M_D^2}{Q^2}} \frac{1}{Q^2} (\omega'-1)^{1-2\alpha_B} \, d\omega' \sim \int_1^{1+\frac{M_D^2}{Q^2}} \frac{1}{Q^2} (\omega'-1)^{\gamma} F_C^2(Q^2) \, d\omega' \qquad \text{(III. 37)}$$

Since $F_c(Q^2) \sim (Q^2)^{\alpha_C - 1}$, it follows that (III. 37) gives γ which controls the threshold behavior of the exclusive channel in terms of α_B and α_C. Matching powers of Q^2 in (III. 37) gives,

$$\gamma = 2(\alpha_C - \alpha_B) - 1 \qquad \text{(III. 38)}$$

Choosing B = proton, C = pion, Eq. (III. 38) predicts that γ should lie between 0 and 1. Since the high ω behavior of γ^* + proton $\rightarrow$ pion + neutron behaves as $\omega^{2\alpha_C - 2} \sim \omega^{-2}$ or ω^{-1}, we expect the fixed Q^2, variable ω behavior of this channel to vary approximately as in Fig. 7.

The same exercise can be carried out for backward electroproduction γ^* + proton $\rightarrow$ nucleon + pion. Then the exclusive cross section should behave as $\sim(\omega'-1)^{-1}$ (!) near $\omega' \approx 1$ and ω^{-3} for large ω (Fig. 8).

In Section IV we try to estimate the numerical magnitude of these cross sections, and further discuss implications of these results.

F. Connection of Photon Fragmentation with Vector Dominance

At $Q^2=0$ the photon fragmentation region is closely related to the e^+e^- annihilation process, according to the ideas of vector meson, in particular ρ^o meson, dominance. Photoproduction processes are reasonably well described by considering the photon to virtually dissociate into a ρ^o which subsequently interacts, either elastically or inelastically. For nonvanishing Q^2, correspondence contrains us to consider this mechanism still operating and to be an integral part of the dynamics.

We begin by reviewing the ρ-dominance idea in photoproduction, using a heavily simplified version of the work of V. N. Gribov.[32] The forward Compton amplitude $\mathscr{T}_T$ for transverse photons (normalized such that Im $\mathscr{T}_T = \nu\sigma_T(Q^2)$) is written,

$$\mathscr{T}_T \sim \frac{f_\rho^2}{(Q^2 + M_\rho^2)^2}\, i\nu\, \sigma_T(\rho p) \qquad \text{(III. 39)}$$

where the denominators come from the energy denominators of the virtual intermediate states of the ρ, according to Fig. 9 (computed with old-fashioned perturbation theory). For large Q^2 many vector intermediate states may be expected to contribute, and

$$\mathscr{T}_T \sim \sum \frac{|\langle 0|j_T|n\rangle|^2\, i\nu\, \sigma_T^{tot}(\{n\}+p)}{(Q^2+m_n^2)^2} \qquad \text{(III. 40)}$$

The matrix elements $\langle 0|j_T|n\rangle$ are what is measured in the colliding-beam process $e^+e^- \to$ hadrons; and assuming the states $\{n\}$ are all absorbed on the proton with about the same cross section, we can sum over all $\{n\}$ of mass m and relate

that matrix element to the total e^+e^- cross section $\sigma_{e\bar{e}}(M^2)$. One gets

$$\sigma_T(Q^2, s) \sim \int_0^{\sim s} dM^2 \, \sigma_{e\bar{e}}(M^2) \left(\frac{M^2}{Q^2+M^2}\right)^2 \bar{\sigma}_T^{\text{tot, hadron}}(M) \qquad \text{(III. 41)}$$

When $M^2 \gtrsim$ (const) s, the longitudinal coherence is lost and the integral should be cut off.[13] If, as supposed in (III. 9), $\sigma_{e\bar{e}} \sim M^{-2}$ for large M^2, we find,

$$\begin{aligned} \sigma_T(Q^2, s) &\sim \sigma_T^{\text{tot, hadron}} \log \omega \\ &\sim \text{const} \log \omega \end{aligned} \qquad \text{(III. 42)}$$

which badly violates scaling.

The picture simply does not work as it stands. Three alternatives, at least, present themselves. The first is to renounce (III. 9), and suppose $\sigma_{e\bar{e}}(M^2) \sim M^{-4}$. This has been analyzed by Sakurai and Schildknecht[33] and is a matter for experiment. The second is that the opacity of the target decreases as M^{-2}, independently of the nature of the state $\{n\}$. We put this option aside temporarily and discuss the third, which is that the opacity decreases sharply for a selected class of states $\{n\}$, namely those possessing high p_T hadron secondaries. The nature of the hadron final states presumed for e^+e^- annihilation in Section III. B are "jets" of hadrons of high momentum, which when boosted into the laboratory frame, possess in general high p_T (Fig. 10). Only when the jet is aligned along the virtual-photon axis is there limited $\langle p_T \rangle$. The probability of such alignment is just a solid-angle factor $\Delta\Omega \sim \langle p_T^2 \rangle / M^2$ and this factor inserted into (III. 41) removes the dilemma. In general, we require that,

$$\sigma_T(Q^2, s) \sim \int^{\sim s} dM^2 \, d\Omega_{c.m.} \, \sigma_{e\bar{e}}(M^2) \left(\frac{M^2}{Q^2+M^2}\right)^2 \sigma_T^{\text{tot, hadron}}(M^2) \, F\left(p_T^2, M^2\right) \qquad \text{(III. 43)}$$

where the opacity factor $F\left(p_T^2, M^2\right)$ is a rapidly falling function of p_T, and where p_T is the transverse momentum of all particles of the jet. For example, it is tempting to make a rough identification of F with the transverse momentum distribution in hadron collisions and the form in (II.21),

$$F\left(p_T^2, M^2\right) \sim \left(\frac{\mu^2}{p_T^2+\mu^2}\right)^n \qquad \text{(III.44)}$$

in order to maintain (according to correspondence) a smooth connection of the p_T distribution with that in the central region.

If we take limited $<p_T>$ and steeply falling p_T distributions in deep-inelastic processes to be required or at least strongly suggested by correspondence, then the above considerations tend to rule out possibilities 1 and 2 above (they would give $d\sigma/dp_T^2 \sim 1/p_T^4$) as well as the "explosion" final-state distribution in e^+e^- annihilation mentioned in Section III.B. Thus, with somewhat increased confidence, we hereafter use the "aligned jet" version of the vector-dominance picture. Remembering that in colliding-beams the distribution in y ($p_\parallel$ is measured along the jet) is as shown in Fig. 11, and that this distribution is now to be taken to be (essentially) the inclusive distribution in the photon fragmentation region, we obtain the picture in Fig. 12 for large ω electroproduction. We observe that there are <u>three</u> fragmentation regions. They are readily identifiable in the parton model as the parton fragmentation region[4,34] ($y \sim y_{max}$), the target fragmentation region ($y \sim y_{min}$) and the hole fragmentation region[8] ($y \sim y_{max} - \ell n\, Q^2$), that being the region in rapidity where the parton struck by the virtual photon was found before being hit. However, we emphasize that our arguments do not rest on the parton model, but on the hypotheses of short-range correlations in rapidity and of correspondence.

G. Coherent Production of Vector States

The information we have obtained on the spectrum and properties of the vector states coupled to the photon allow us to infer the nature of their coherent production. The probability of the photon being a vector hadron state of mass M was found (Eq. (III.43)) to be,

$$dP(M^2) \sim \sigma_{e\bar{e}}(M^2) \left(\frac{M^2}{Q^2+M^2}\right)^2 dM^2 \qquad \text{(III.45)}$$

The probability these states scatter elastically may be assumed again to be $\sim\sigma_{el}/\sigma_{tot} \sim$ const (as for typical hadron processes), multiplied by the opacity factor $\sim \langle p_T^2 \rangle / M^2$ which gives the probability the jet axis in the state $\{n\}$ is aligned along the direction of the virtual photon. Thus,

$$\frac{d\sigma_{coh}(Q^2)}{dM^2} \sim \frac{\text{const}}{(Q^2+M^2)^2} \qquad \text{(III.46)}$$

This expression might be made more realistic by the introduction of a mass spectrum $\rho(M^2)$,

$$\frac{d\sigma_{coh}(Q^2)}{dM^2} \sim \frac{\rho(M^2)}{(Q^2+M^2)^2} \qquad \text{(III.47)}$$

The function ρ is expected to have resonant bumps at the prominent vector meson states (ρ, ω, ϕ) and should approach a constant for large M^2 (Fig. 13). From (III.47) the total diffraction contribution to $\sigma_{tot}(Q^2)$ becomes

$$\sigma_{coh}(Q^2) \sim \frac{1}{Q^2+M_\rho^2} + \ldots \qquad \text{(III.48)}$$

So, the mass which determines the onset of scaling for this piece of the cross section is a small number $\sim M_\rho^2$ (precocious scaling). Notice that for real photons,

$$\frac{d\sigma_{coh}(0)}{dM^2} \sim \frac{1}{M^4} \qquad \text{(III.49)}$$

and low mass states (e.g., the ρ^0) are expected to dominate, while for large Q^2, $\langle M^2 \rangle \sim Q^2$. Therefore, in this picture the electroproduction of the prominent low mass vector states are an integral part of the scaling phenomenon, although they play an increasingly unimportant role as Q^2 grows. It will be interesting to investigate coherent electroproduction from nuclei to see whether these expectations are in the right directions. A crucial test is the prediction that for large M^2, the hadrons produced have low $\langle p_T \rangle$ and low multiplicity ($\bar{n} \sim C \ell n\, M^2$).

H. The Central Plateau in the Photon Fragmentation Region

In pure hadronic inclusive reactions the single hadron distribution function possesses a flat plateau of length $\sim \ell n\, s$. In particular, if one imagines a reaction $A+B \to C+$anything in the c.m.s., then the principle of short-range correlations implies that the height of the plateau to the right of y=0 matches the height of the plateau to the left of y=0 even if $A \neq B$.

It is now natural to ask whether the inclusive distribution for $\gamma^* + B \to C +$ anything is equally simple. The complicating fact is that the central plateau in the photon fragmentation region of length $\sim \ell n\, Q^2$ is separated from the other plateau by the hole fragmentation region. It is not a priori clear that the average height of the photon plateau should match onto the height of the central plateau.[35] To give a rough answer to this question suppose that the average multiplicity in the central region is $\bar{n} \sim C_1 \ell n\, \omega$ and the average multiplicity in the photon fragmentation region is $\bar{m} \sim C_2 \ell n\, Q^2$. There is certainly no model independent connection between the densities C_1 and C_2. Therefore, it is necessary to construct a simple model of hadron production in both regions of phase space and see whether, in the limited context of the model, the correspondence argument provides a relation.

Consider the following model: let the cross section for the production of n hadrons in the central region and m hadrons in the photon fragmentation region be,

$$\sigma_{n,m} = \frac{1}{Q^2}\left(\frac{\bar{n}^n}{n!}\, e^{-\bar{n}}\right)\left(\frac{\bar{m}^m}{m!}\, e^{-\bar{m}}\right) \qquad \text{(III.50)}$$

In other words, we suppose that the emission of hadrons in one region is independent of the emission of hadrons in the other region and that within each region the emission of hadrons are statistically independent.[4,36] Approximately, such a formula is expected in models possessing short-range correlations only. By construction the total cross section scales,

$$\sigma_{tot} = \sum_{n,m} \frac{1}{Q^2}\left(\frac{\bar{n}^n}{n!}\, e^{-\bar{n}}\right)\left(\frac{\bar{m}^m}{m!}\, e^{-\bar{m}}\right) \qquad \text{(III.51)}$$

$$\sigma_{tot} = \frac{1}{Q^2}$$

The quantities $\bar{n}$ and $\bar{m}$ may be estimated by equating $\sigma_{0,0}$ with the exclusive channel $\gamma^* + B \to C + D$ given by Eq. (III.25). So,

$$\sigma_{0,0} = \frac{1}{Q^2}\, e^{-(\bar{n}+\bar{m})} \sim \frac{1}{Q^2}\, s^{2(\alpha_C - 1)} \qquad \text{(III.52)}$$

Therefore,

$$\bar{n}+\bar{m} = C_1 \ln \omega + C_2 \ln Q^2 = 2(1-\alpha_C) \ln s \qquad \text{(III.53)}$$

which requires that,

$$C_1 = C_2 \qquad \text{(III.54)}$$

So, for high ω and Q^2, the single hadron inclusive spectrum (averaged over particle types) should be roughly flat over the whole rapidity axis (Fig. 14).

IV. SEMIQUANTITATIVE ESTIMATES OF CROSS SECTIONS

In an attempt to convince ourselves (if not the reader) that the preceding considerations have some content, we have endeavored to put in some numbers and make order-of-magnitude guesses for some of the cross sections we discuss. These are presented in turn below.

A. $pp \to \pi^0 + \text{Hadrons}$

Following the arguments in the text (in particular, the discussion preceding Eq. (II. 20)), we choose the form for $\pi p \to \pi^0 + \text{hadrons}$ to be,

$$E\frac{d^3\sigma}{dp^3} = N\left(\frac{\mu^2}{p_\perp^2+\mu^2}\right)^4\left(1-\frac{p}{p_{max}}\right)^3 \qquad \text{(IV. 1)}$$

From the fit of Gunion, Brodsky, and Blankenbecler[5,6] to elastic πp scattering,

$$s^8\frac{d\sigma}{dt} \approx 5\times 10^4 \text{ mb - GeV}^{14} \qquad \text{(IV. 2)}$$

and from the inclusive-exclusive connection we set,

$$s^8\frac{d\sigma}{dt} \approx 64\pi N\mu^8 M^8 \qquad \text{(IV. 3)}$$

with $M \approx 2$ GeV, the maximum missing mass in Eq. (II. 14). From the inclusive distribution for π^+ in the "central plateau", integrated over $p_\perp$, we find,

$$\frac{d\sigma}{dy} = E\frac{d\sigma}{dp} \approx 12 \text{ mb} \approx \frac{\pi N\mu^2}{3} \qquad \text{(IV. 4)}$$

Equations (IV. 3) and (IV. 4) can be solved for N and μ^2, thereby determining the inclusive distribution in pion-nucleon collisions. For nucleon-nucleon collisions, we expect the same form as (IV. 1), with the same N and μ^2, but we cannot determine the exponent n for the factor $\left(1-\frac{p}{p_{max}}\right)^n$. It is probably $\gtrsim 3$, and in Fig. 15 we plot Eq. (IV. 1) for the choice n=3. The result is within an order of magnitude of the more detailed estimates of Gunion, Brodsky, and Blankenbecler.

However, for the choice of μ^2 made, it turns out that

$$\langle p_\perp^2 \rangle \approx 450 \text{ MeV} \quad .$$

Furthermore, the result is quite sensitive to our choice of M. Therefore, our calculated curve should not be taken very seriously.

B. pp → p + Hadrons

These doubts increase even further when the nucleon spectrum is calculated. Using only the inclusive-exclusive connection with elastic scattering, fitted to the form

$$s^{11} \frac{d\sigma}{dt} \cong 5 \times 10^{12} \, \mu b - \text{GeV}^{20} \qquad \text{(IV.5)}$$

we can calculate an inclusive distribution of protons at large $p_\perp$. Using the same connection as before, with M = 2 GeV, we find

$$E \frac{d^3\sigma}{dp^3} \approx 6 \times 10^{-2} \left(\frac{2.5 \text{GeV}}{p_\perp} \right)^{12} \left(1 - \frac{p}{p_{max}} \right)^4 \text{mb/GeV}^2 \quad . \qquad \text{(IV.6)}$$

This, if believed, would imply at $p_T \sim 2$ GeV a flux of nucleons greater than what is measured at 90° at $p_T = 0$! The formula as it stands is certainly wrong at low p_T. At $p_T \sim 5 - 10$ GeV/c, the p/π ratio comes out to be $\sim 1 - 10$.

The most likely conclusion to be drawn is that this application of correspondence is much too naive. Yet, the calculation does raise interesting questions. First, what does the model of Gunion, Brodsky, and Blankenbecler really imply for the size and shape of the proton spectrum? And secondly, is it conceivable that a more realistic interpolation would leave the p/π ratio large at $p_T \sim 5 - 10$ GeV/c? And finally, of course, what does experiment say?

C. Hadron Distributions in e^+e^- Annihilation

Given the constraints we have deduced in Section III, the inclusive distribution of $\pi^{\pm}$ in e^+e^- annihilation (via one photon) is fairly well determined. We plot the distribution for π^+ in Fig. 16, given that

(a) $\bar{n}_{\pi^+} \to C_{\pi^+} \log Q^2$ $(Q^2 \to \infty)$, with $C_{\pi^+} \approx 0.5$.

(b) The mean fraction of the virtual-photon energy Q given to π^+ mesons is ~ 0.3.

(c) $F_{\pi}(Q^2) \to Q^{-2}$, $Q^2 \to \infty$.

These conditions determine, in Fig. 16, the intercept at $p/p_{max} = 0$, the area under the curve, and the power behavior near x=1, respectively.

The production of $\bar{p}$ (or $\bar{n}$) can similarly be estimated. At asymptotic energies we obtain Fig. 17, assuming

(a) $\bar{n}_{\bar{p}} \to .025 \log Q^2$ $(Q^2 \to \infty)$ corresponding to an asymptotic $\bar{p}/\pi^-$ ratio of ~5% in the central plateau. This is a number of the order observed in the CERN-ISR experiments.[37]

(b) $F_N(Q^2) \to Q^{-4}$ $(Q^2 \to \infty)$, as appears to be the case for spacelike Q^2.

At realistic energies, the large nucleon mass implies important corrections to the asymptotic curve. We try to simulate this by multiplying by $\beta^3 = (p/E)^3$, which creates, for small β, a uniform phase-space density of $\bar{p}$'s. The corrections for three typical energies are shown in Fig. 17. From these curves we can estimate the fraction of events containing a $\bar{p}$, as a function of Q^2. This is plotted in Fig. 18. From the Frascati measurement near threshold,[38] at $Q^2 \sim 4.4$ GeV^2, we see that our estimate at low Q^2 is probably too conservative.

Production of a strange baryon Y may be dealt with in a similar way. One may simply scale the distributions in Figs. 17 and 18 by replacing $\sqrt{Q^2}$ by $\sqrt{Q^2}\ M_p/M_Y$. This substitution keeps the value of β fixed for a given p/p_{max}.

Of course the overall normalization of the inclusive distribution may well vary with particle type, decreasing as the strangeness increases.

D. Exclusive Electroproduction of a π^+

The total transverse cross section for the reaction $\gamma^* p \to \pi^+ n$ at large ω was suggested to be roughly,

$$\sigma^T_{\gamma^* p \to \pi^+ n} \sim \frac{\text{const}}{Q^2 s^2} \quad .$$

We write (for $\omega >> 1$),

$$\sigma^T_{\gamma^* p \to \pi^+ n} \approx (50 \text{ mb}) \left(\frac{M_\rho^2}{Q^2 + M_\rho^2} \right) \frac{(1 \text{ GeV}^4)}{s^2} \tag{IV.7}$$

which joins smoothly onto photoproduction[39] at $Q^2=0$. For any ω it follows from Eqs. (III.27), (III.35), and (III.38) that

$$\sigma^T_{\gamma^* p \to \pi^+ n} \approx \frac{1}{Q^6} F(\omega) \tag{IV.8}$$

where

$$\begin{aligned} F(\omega) &\approx C(\omega - 1) && \text{for } \omega \approx 1 \\ F(\omega) &\approx (7 \times 10^{-2}) \omega^{-2} && \text{for } \omega >> 1 \quad . \end{aligned} \tag{IV.9}$$

For $s \lesssim 2 - 3 \text{ GeV}^2$, the total electroproduction cross section is dominated by the two-body channels $\pi^+ n$ and $\pi^o p$; for $Q^2 \gtrsim 1 \text{ GeV}^2$,

$$\sigma^T_{\text{tot}}(Q^2, \omega) \approx \frac{4\pi^2 \alpha}{Q^2} (\nu W_2) \approx \frac{.05}{Q^2} (\omega' - 1)^3 \tag{IV.10}$$

where

$$\omega' = 1 + \frac{s}{Q^2} \lesssim 3 \quad .$$

We join the form (IV.10) onto (IV.7) at $Q^2 = Q_0^2$, $s = s_0$, $\omega' < 2$, recognizing that this procedure is quite sensitive to this choice of parameters, in particular the

value of s_0. Thus, assuming at this point $\sigma^T_{\gamma^* p \to \pi^+ n} \sim \frac{1}{2}\sigma^T_{tot}$, we obtain from (IV.9),

$$F(\omega') \approx C(\omega'-1) \approx \frac{1}{2} Q_0^6 \left(\frac{.05}{Q_0^2}\right) (\omega'-1)$$

or

$$C = .025\ s_0^2 \qquad \text{(IV.11)}$$

We take $s_0 \approx 2\ \text{GeV}^2$, obtaining

$$\sigma^T_{\gamma^* p \to \pi^+ n} \approx \frac{0.1}{Q^6} (\omega'-1) \quad , \qquad \omega' \approx 1 \qquad \text{(IV.12)}$$

From (IV.9) and (IV.12) we may now estimate σ^T in general; it is plotted in Fig. 19. We again plot $\sigma^T(Q^2, s)$ for various Q^2 in Fig. 20.

Backward electroproduction $\gamma^* p \to n\pi^+$ may be easily estimated from forward electroproduction. For large ω, it follows from Eqs. (III.25) and (III.30) that,

$$\frac{\sigma_{\gamma^* p \to n\pi^+}}{\sigma_{\gamma^* p \to \pi^+ n}} \sim \frac{1}{s} \qquad \text{(IV.13)}$$

For $s \lesssim 3$, the ratio should evidently be $\sim$ unity. Therefore, a smooth interpolation is provided by (IV.13), now at <u>all</u> ω. This result also follows from the more detailed considerations in the preceding section. We therefore guess that <u>at fixed s the backward/forward ratio is independent of Q^2</u>.

Indeed, if we examine the ratio

$$\frac{\sigma_{\text{exclusive}}(Q^2, s)}{\sigma_{tot}(Q^2, s)} \approx \frac{\frac{1}{Q^6} F(\omega)}{\frac{0.3}{Q^2} \nu W_2} \approx \frac{1}{s^2} G(\omega) \qquad \text{(IV.14)}$$

we find that with our parameters,

$$G(\omega) = \begin{cases} 2\ , & \omega \approx 1 \\ 0.7\ , & \omega >> 1 \end{cases} \qquad \text{(IV.15)}$$

That is, at a given value of s, the ratio of the cross section for an exclusive channel to the total cross section has no systematic variation with Q^2. It also follows that as a function of s, the ratio $\sigma_{\text{exclusive}}(Q^2, s)/\sigma_{\text{tot}}(Q^2, s)$ is approximately Regge-behaved for all $s \gg M^2$. Finally, inasmuch as both the normalized exclusive channels and the mean multiplicity at a given s should not vary systematically with Q^2, it is likely that the prong distribution (i.e., $\sigma_n/\sigma_{\text{tot}}$ vs. n) at fixed s shows no systematic variation with Q^2.

V. SUMMARY AND CONCLUSIONS

The detailed consequences of this paper, especially in the previous section, must be treated with great caution. Very little dynamics was put in, and the results should be viewed as semiquantitative at best. And some of the results appear baffling to us in the context of our present views of deep-inelastic dynamics. These include:

(a) The connection, albeit vague, of asymptotic behavior of elastic electromagnetic form factors to Regge trajectories, $F(Q^2) \sim (Q^2)^{\alpha-1}$.

(b) The equality of the height of the "current-plateau" with the "hadronic plateau" in inclusive electroproduction.

(c) The Q^2-independence of the ratio of exclusive to total electroproduction cross sections at fixed s and its implication that a Regge form for that ratio is applicable for all $s \gg M^2$, even when ω is small and we expect a Regge description to break down.

(d) The mysterious mechanism which aligns the vector-dominant "jets" along the virtual photon direction in high Q^2, high ω electroproduction of massive vector states.

All of these results may be tested, not only in electroproduction, but also in high-energy neutrino processes. And again we wish to emphasize that it is not only these specific applications we have presented, but a method, the use of correspondence, which is applicable to a large variety of models of high-energy phenomena. We believe that, with few exceptions, they all should be made to pass the tests of correspondence we have studied here, and that such tests will give useful information with regard to their internal self-consistency.

REFERENCES

1. R. Dolen, D. Horn and C. Schmid, Phys. Rev. 166, 1768 (1968).
2. This has been emphasized by H. Harari; see e. g. Proceedings of the International Conference on Duality and Symmetry in Hadron Physics, ed. E. Gotsman, Weizmann Science Press of Israel, Jerusalem, 1971.
3. N. Bohr, Zeitschrift fur Physik 2, 423 (1920).
4. R. P. Feymman, invited paper at the Third Topical Conference in High Energy Collisions of Hadrons, Stony Brook, New York, September 1969; Phys. Rev. Letters 23, 1415 (1969); unpublished.
5. J. F. Gunion, S. J. Brodsky and R. Blankenbecler, Phys. Letters 39B, 649 (1972).
6. R. Blankenbecler, S. J. Brodsky and J. F. Gunion, Phys. Letters 42B, 461 (1972).
7. J. D. Bjorken, invited paper at the Conference on Particle Physics, Irvine, California, December 3-4, 1971; SLAC-PUB-1017, February 1972.
8. J. D. Bjorken, SLAC-PUB-1114, September 1972 (to appear in Comments and Addenda to Phys. Rev.).
9. A plethora of references on this subject are found in the review of W. R. Frazer, L. Ingber, C. H. Mehta, C. H. Poon, D. Silverman, K. Stowe, P. D. Ting and H. J. Yesian, Reviews of Modern Phys. 44, 284 (1972).
10. R. C. Hwa, Phys. Rev. Letters 26, 1143 (1971); M. Jacob and R. Slansky, Phys. Rev. D5, 1847 (1972).
11. A. H. Mueller, Phys. Rev. D2, 2963 (1970).
12. We hope the notation is familiar to the reader, If not, see F. Gilman, Proceedings of the Fourth International Conference on Electron and Photon Interactions at High Energy, Daresbury, England, 1969.

13. J. D. Bjorken, invited paper at the 1967 International Symposium on Electron and Photon Interactions at High Energies, Stanford Linear Accelerator Center, Stanford, California, September 5-9, 1967. See also H. T. Nieh, Phys. Rev. D1, 3161 (1970).

14. J. D. Bjorken, Phys. Rev. Letters 16, 408 (1966).

15. S. Adler, Phys. Rev. 143, 1144 (1966).

16. S. D. Drell and T. M. Yan, Phys. Rev. Letters 24, 181 (1970).

17. E. D. Bloom and F. J. Gilman, Phys. Rev. Letters 25, 1140 (1970).

18. See for example J. D. Bjorken, Phys. Rev. 148, 1467 (1966); V. N. Gribov, B. L. Ioffe, and I. Ya. Pomeranchuk, Phys. Letters 24B, 554 (1967).

19. See for example the review of e^+e^- data by D. M. Ritson, invited paper at the Third International Conference on Experimental Meson Spectroscopy at the University of Pennsylvania, Philadelphia, Pennsylvania, April 27-29, 1972; SLAC-PUB-1043, March 1972.

20. S. D. Drell and T.-M. Yan, Phys. Rev. Letters 24, 855 (1970).

21. C. G. Callan and D. J. Gross, IAS Preprint, March 1972.

22. T. T. Chou and C. N. Yang, Phys. Rev. D4, 2005 (1972).

23. J. D. Bjorken and S. J. Brodsky, Phys. Rev. D1, 1416 (1970).

24. K. Moffeit, J. Ballam, G. Chadwick, M. Della-Negra, R. Gearhart, J. Murray, P. Seyboth, C. Sinclair, I. Skillicorn, H. Spitzer, G. Wolf, H. Bingham, W. Fretter, W. Podolsky, M. Rabin, A. Rosenfeld, R. Windmolders, G. Yost, and R. Milburn, Phys. Rev. D5, 1603 (1972).

25. J. D. Stack, Phys. Rev. Letters 28, 57 (1972).

26. V. Alles Borelli et al., Phys. Letters 40B, 433 (1972). G. Barbiellini et al., University of Rome preprint 420, to be published.

27. Since the exchanged nucleon (Fig. 6) is off-shell ($t \approx 0$), this is not quite the physical nucleon form factor. Luckily, little such ambiguity occurs for the pion form factor (III.31).

28. R. A. Brandt, Phys. Rev. D1, 2808 (1970); H. Pagels, Phys. Letters 34B, 299 (1971); M. Elitzur, Phys. Rev. D3, 2166 (1971).

29. Supporting arguments based on generalized vector dominance will be given in Sec. III.F.

30. J. Weis, Nuclear Physics 40B, 562 (1972).

31. Y. Frishman, V. Rittenberg, H. R. Rubinstein, and S. Yankieowicz, Phys. Rev. Letters 26, 798 (1971).

32. V. N. Gribov, "High Energy Interactions of Gamma Quanta and Electrons with Nuclei," preprint from the Fourth Winter Seminar on the Theory of the Nucleus and the Physics of High Energies, February 5-17, 1969, Ioffe Institute of Engineering Physics, Acad. Sci. USSR. See also S. J. Brodsky and J. Pumplin, Phys. Rev. 182, 1794 (1969); K. Gottfried and D. R. Yennie, Phys. Rev. 182, 1595 (1969).

33. J. J. Sakurai and D. Schildknecht, Phys. Letters 40B, 121 (1972).

34. S. M. Berman, J. D. Bjorken, and J. B. Kogut, Phys. Rev. D4, 3388 (1971); R. P. Feynman, Photon Hadron Interactions, W. A. Benjamin, New York (1972); M. Gronau, F. Ravndal, and Y. Zarmi, Caltech preprint CALT-68-367 (submitted to Nuclear Physics B).

35. This has been considered by R. Cahn, J. Cleymans, and E. W. Colglazier, SLAC-PUB-1136 (to be published).

36. G. F. Chew and A. Pignotti, Phys. Rev. 176, 2112 (1968).

37. J. C. Sens, Proceedings of the Fourth International Conference on High Energy Collisions, Oxford, U.K., April 5-7, 1972, to be published.

38. C. Bernardini, report to the 1971 International Symposium on Electron and Photon Interactions at High Energies, Cornell University, Ithaca, New York, August 23-27, 1971, Laboratory of Nuclear Sciences, Cornell University (1972).

39. For example, see R. Diebold, Proceedings of the Boulder Conference on High Energy Physics, Boulder, Colorado (1969).

FIGURE CAPTIONS

1. Structure of a typical inclusive distribution of secondary hadrons as a function of rapidity y.
2. Typical momentum spectrum of secondary particles, as observed in a single-particle inclusive spectrum.
3. Example of an inclusive spectrum which apparently violates correspondence. The magnitude of the spike at $p \approx p_{max}$, associated with diffraction dissociation, is as $p_{max} \to \infty$ large compared to the continuum in the resonance region, violating the assumption made for the inclusive-exclusive connection.
4. Kinematical regions for deep-inelastic scattering.
5. Structure of the inclusive distribution of hadrons for deep-inelastic electroproduction.
6. Diagram illustrating exchange of Reggeon α in deep-inelastic exclusive electroproduction.
7. General structure of total cross section for the process $\gamma^* p \to \pi^+ n$.
8. General structure of the total backward-scattering cross section $\gamma^* p \to n\pi^+$.
9. ρ-dominance diagram for the forward Compton scattering amplitude of a virtual photon γ^*.
10. Possible high-mass jets of high $p_\perp$ produced by virtual photons.
11. Inclusive rapidity-distribution of hadrons in e^+e^- single-photon annihilation. The z axis is taken to be along the direction of motion of the hadron of highest energy, as measured in the center-of-mass frame.
12. Fragmentation regions for electroproduction at very large ω and large Q^2.
13. Spectrum of vector states coupled to the virtual photon, proportional to $\sigma(e^+e^- \to \text{hadrons})/\sigma(e^+e^- \to \mu^+\mu^-)$.

14. Inclusive production of π at 90° in pp collisions. The solid lines are our interpolations based on Eq. (IV.1). The dashed lines are the detailed calculations of Gunion, Brodsky, and Blankenbecler. The ? curve is our estimate of inclusive production of protons in 90° pp collisions, according to Eq. (IV.6).

15. Expected inclusive distribution of π^+ for the reaction $e^+e^- \rightarrow \pi^+ +$ hadrons.

16. Expected inclusive distribution of $\bar{p}$ (or p) for the reaction $e^+e^- \rightarrow \bar{p} +$ hadrons. The dotted curves include a phase-space correction factor of $\beta^3 = (p/E)^3$.

17. Estimated fraction of $e^+e^- \rightarrow$ hadrons events containing a $\bar{p}$ in the final state. The experimental point comes from the measurement of $e^+e^- \rightarrow p\bar{p}$ at Frascati, and omits any contribution from $e^+e^- \rightarrow \bar{p}N\pi$.

18. Estimated cross section σ_T for the process $e^-p \rightarrow e^-\pi^+n$ at large Q^2 and s.

19. Estimated cross section σ_T for the process $e^-p \rightarrow e^-\pi^+n$ as a function of s for $Q^2 = 1, 3,$ and 10 GeV^2.

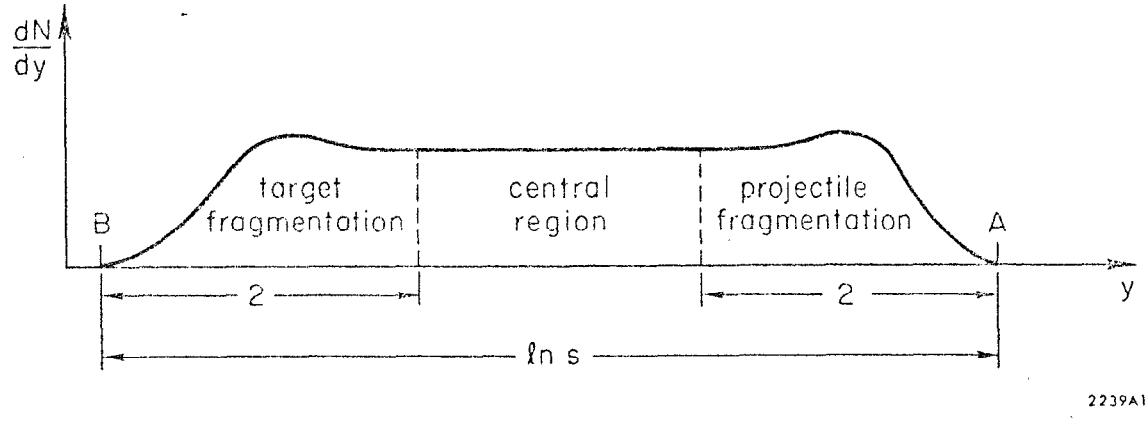
dN/dy
target fragmentation
central region
projectile fragmentation
B
A
y
2
2
ℓn s
2239A1

Fig. 1

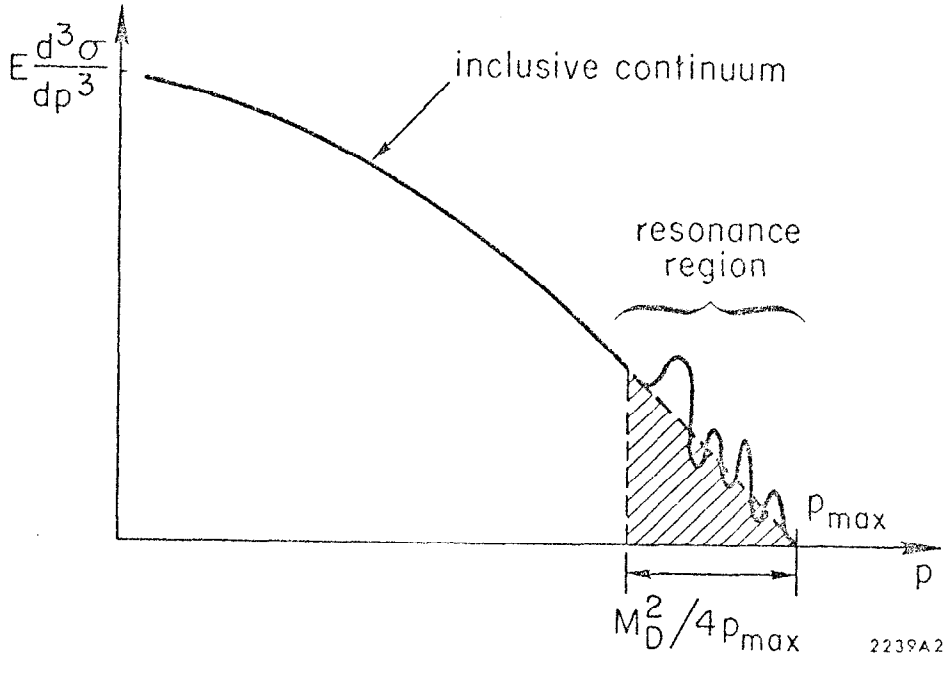
$E\frac{d^3\sigma}{dp^3}$
inclusive continuum
resonance region
p_{max}
p
$M_D^2/4p_{max}$
2239A2

Fig. 2

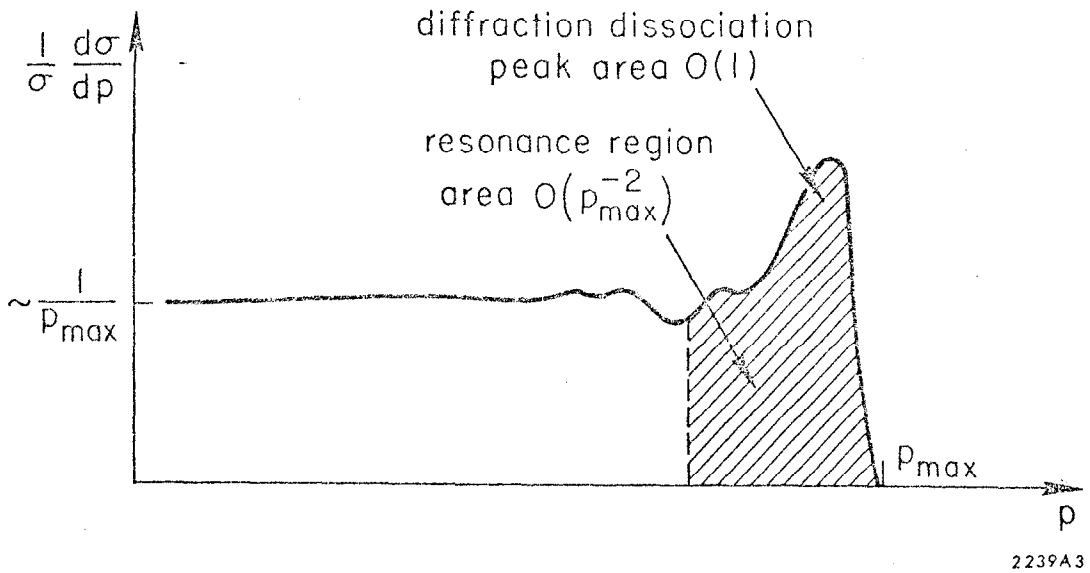
$\frac{1}{\sigma}\frac{d\sigma}{dp}$
diffraction dissociation
peak area O(1)
resonance region
area $O(p_{max}^{-2})$
$\sim \frac{1}{p_{max}}$
p_{max}
p
2239A3

Fig. 3

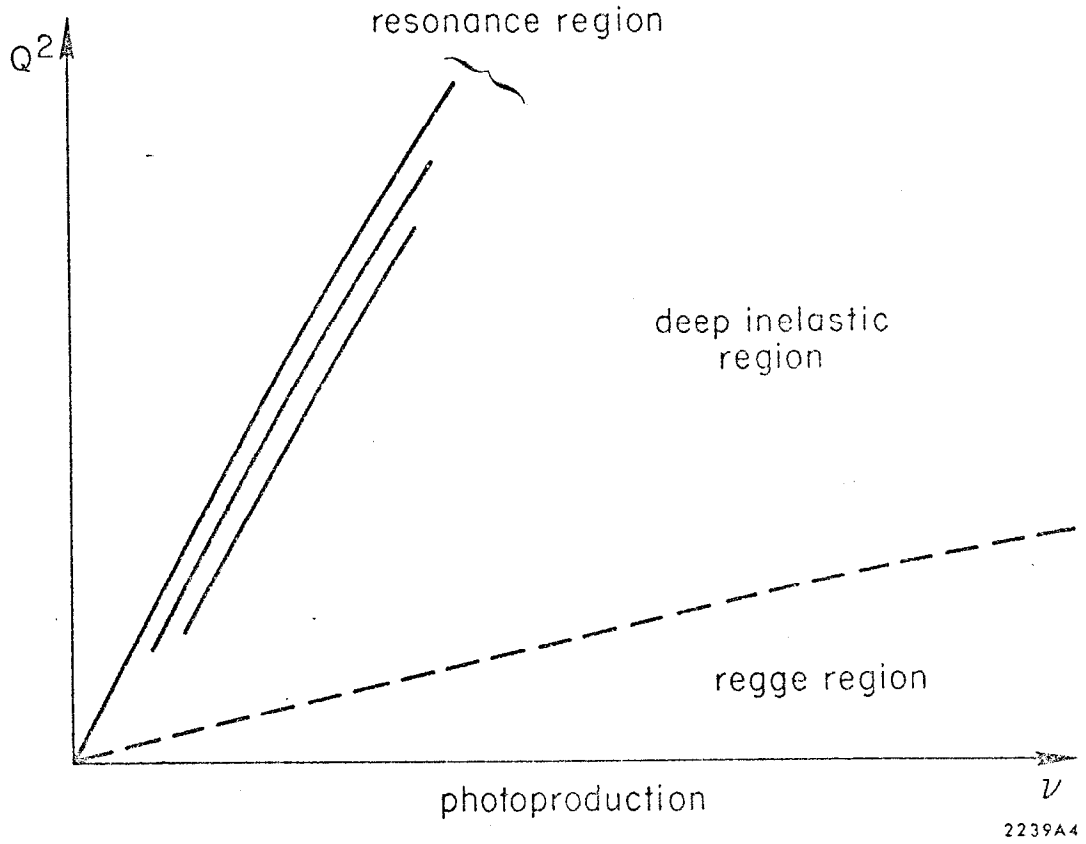
resonance region
Q^2
deep inelastic region
regge region
photoproduction
ν
2239A4

Fig. 4

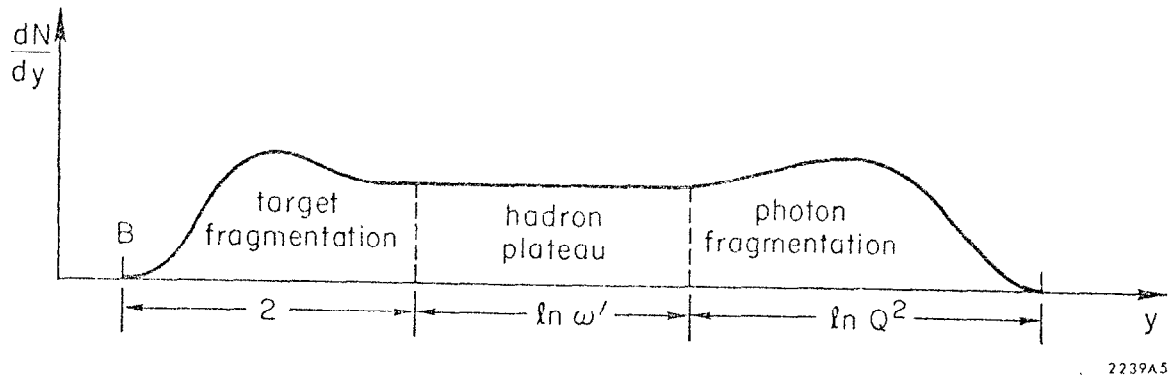
dN/dy
B
target fragmentation
hadron plateau
photon fragmentation
2
ln ω'
ln Q²
y
2239A5

Fig. 5

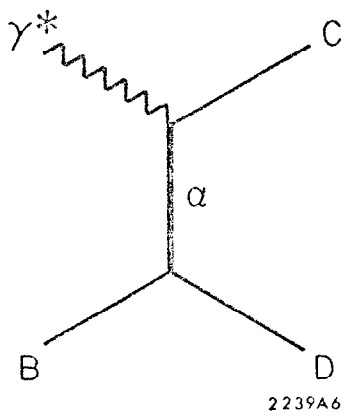

Fig. 6

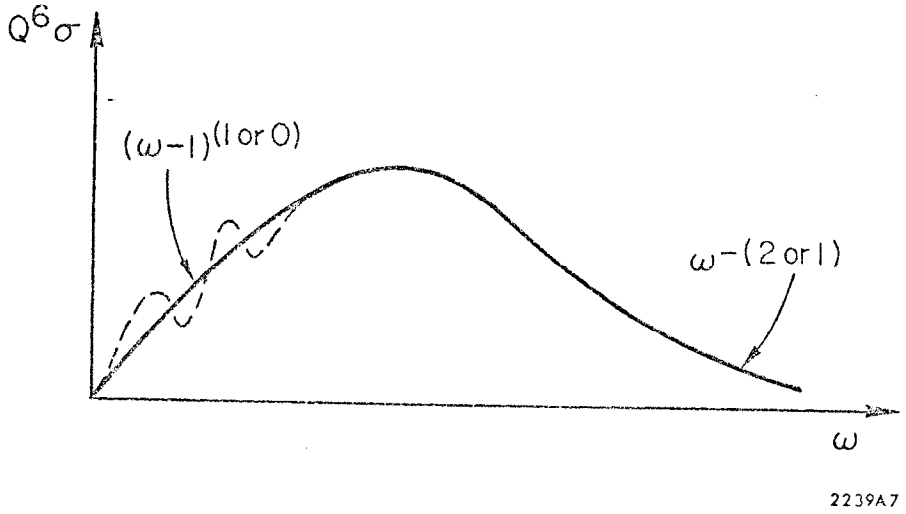

Fig. 7

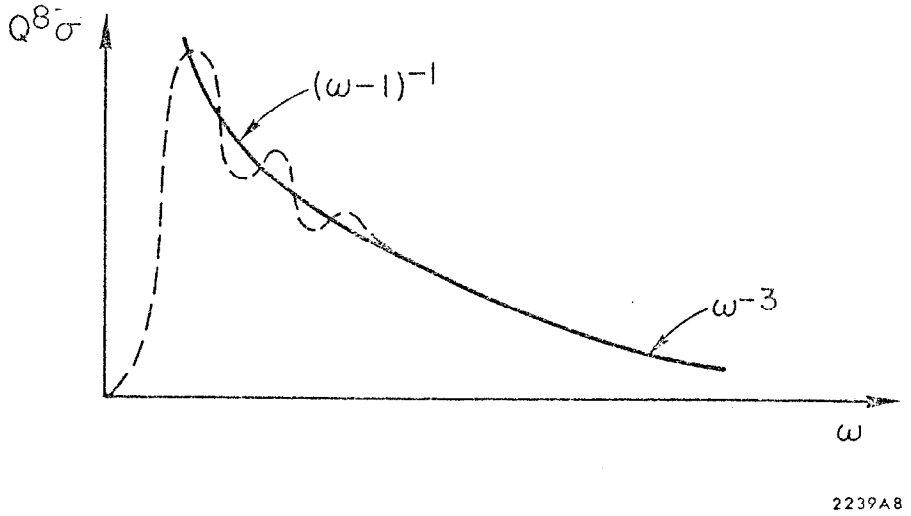

Fig. 8

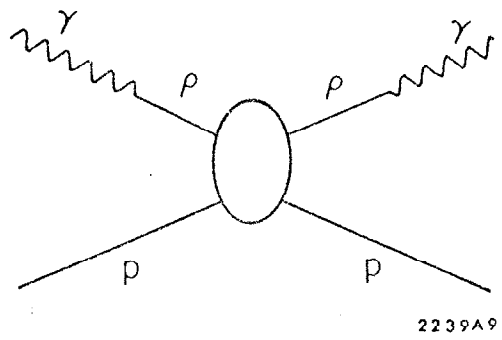

Fig. 9

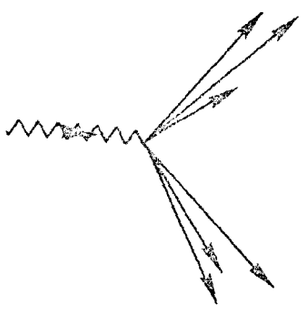

2239A10

Fig. 10

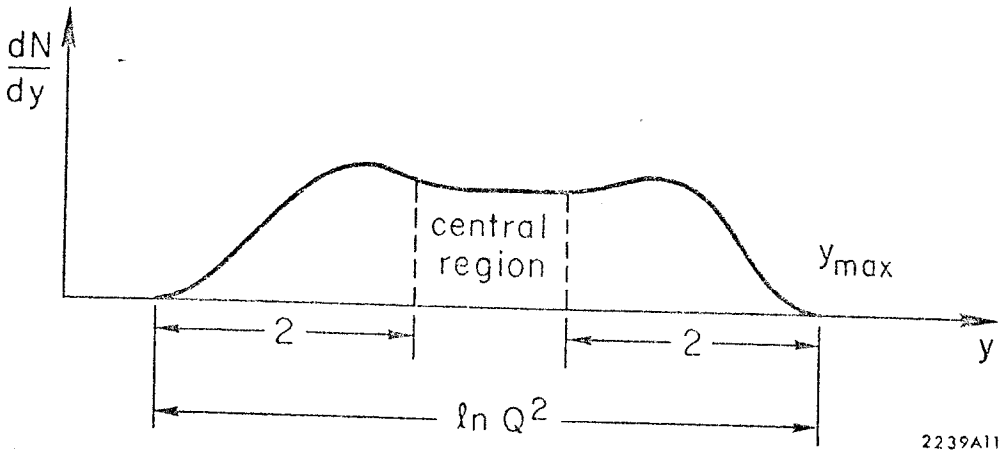

Fig. 11

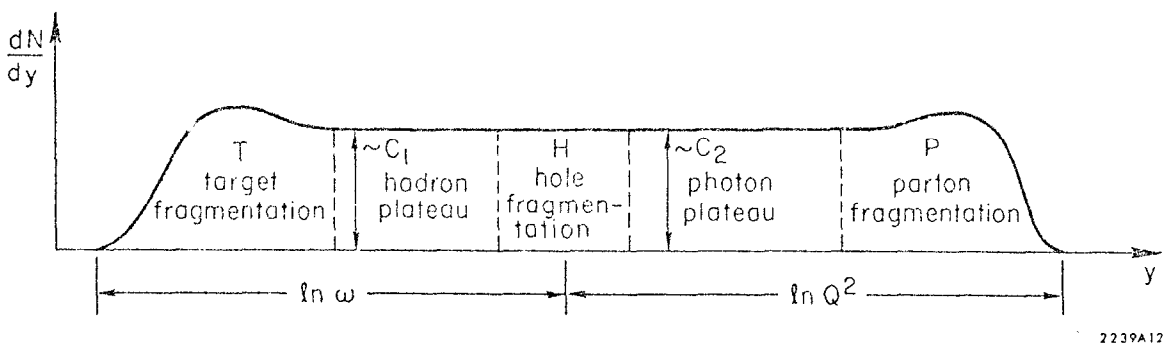
dN/dy
T
target
fragmentation
~C1
hadron
plateau
H
hole
fragmen-
tation
~C2
photon
plateau
P
parton
fragmentation
y
ln ω
ln Q2
2239A12

Fig. 12

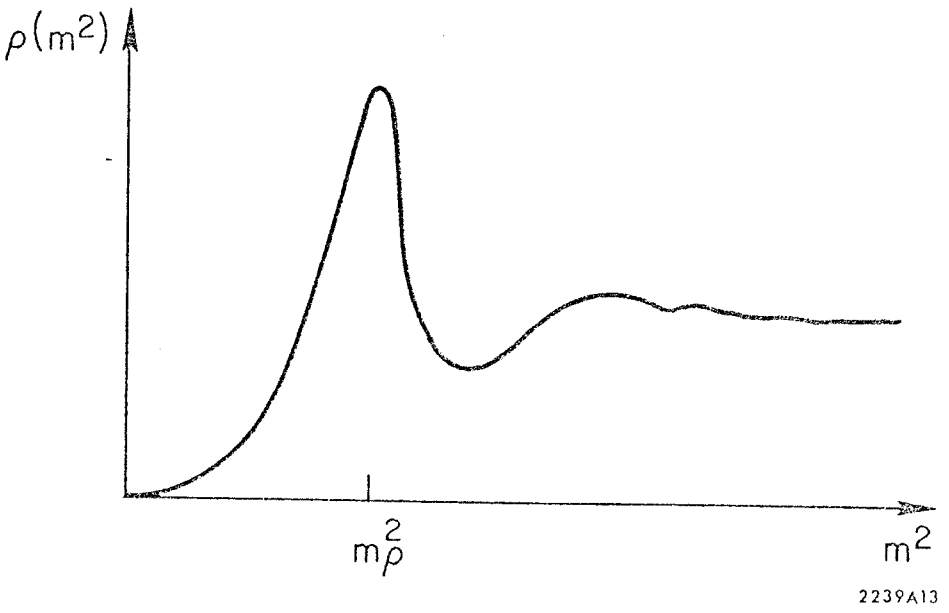

Fig. 13

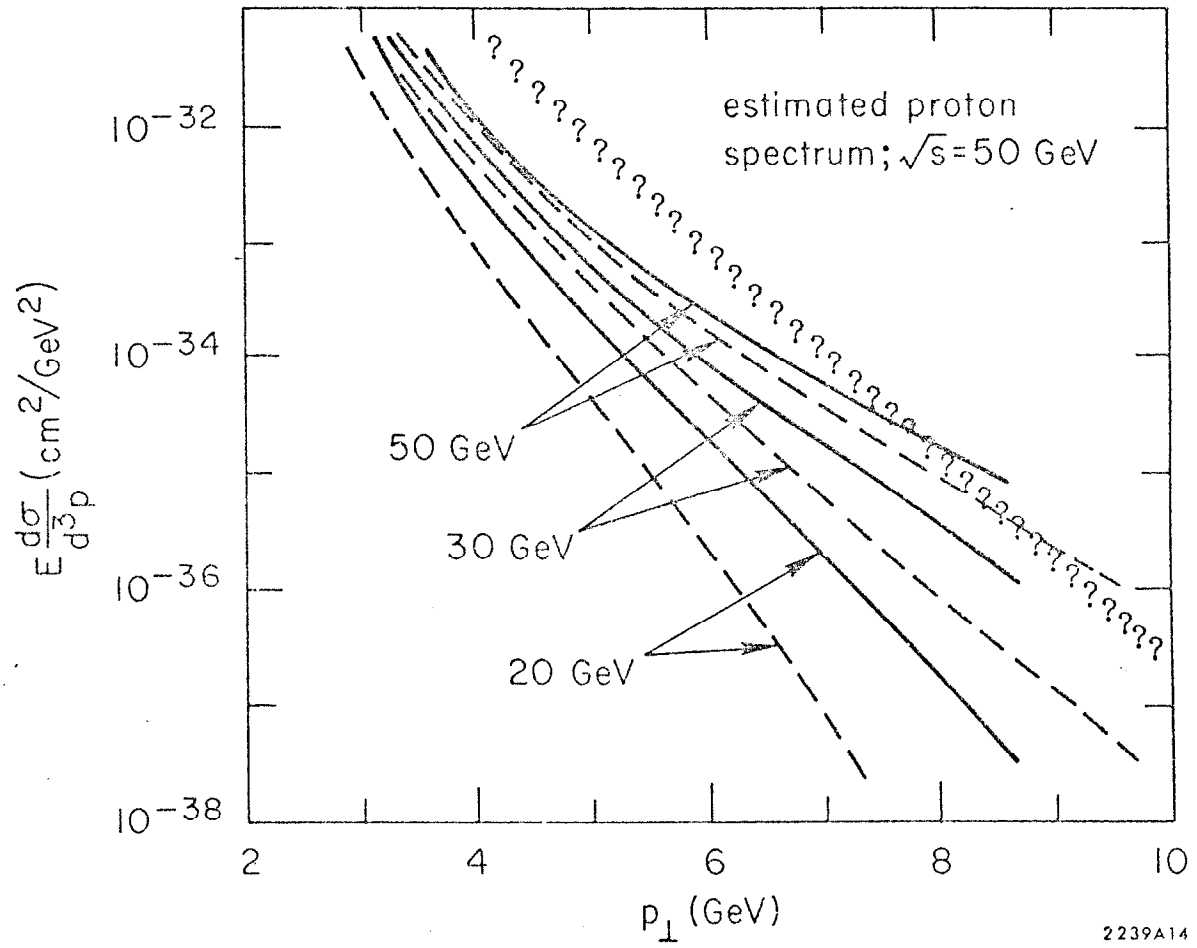
estimated proton
spectrum; $\sqrt{s}$=50 GeV
50 GeV
30 GeV
20 GeV
$E\frac{d\sigma}{d^3p}$ (cm^2/GeV^2)
10^{-32}
10^{-34}
10^{-36}
10^{-38}
2
4
6
8
10
$p_\perp$ (GeV)
2239A14

Fig. 14

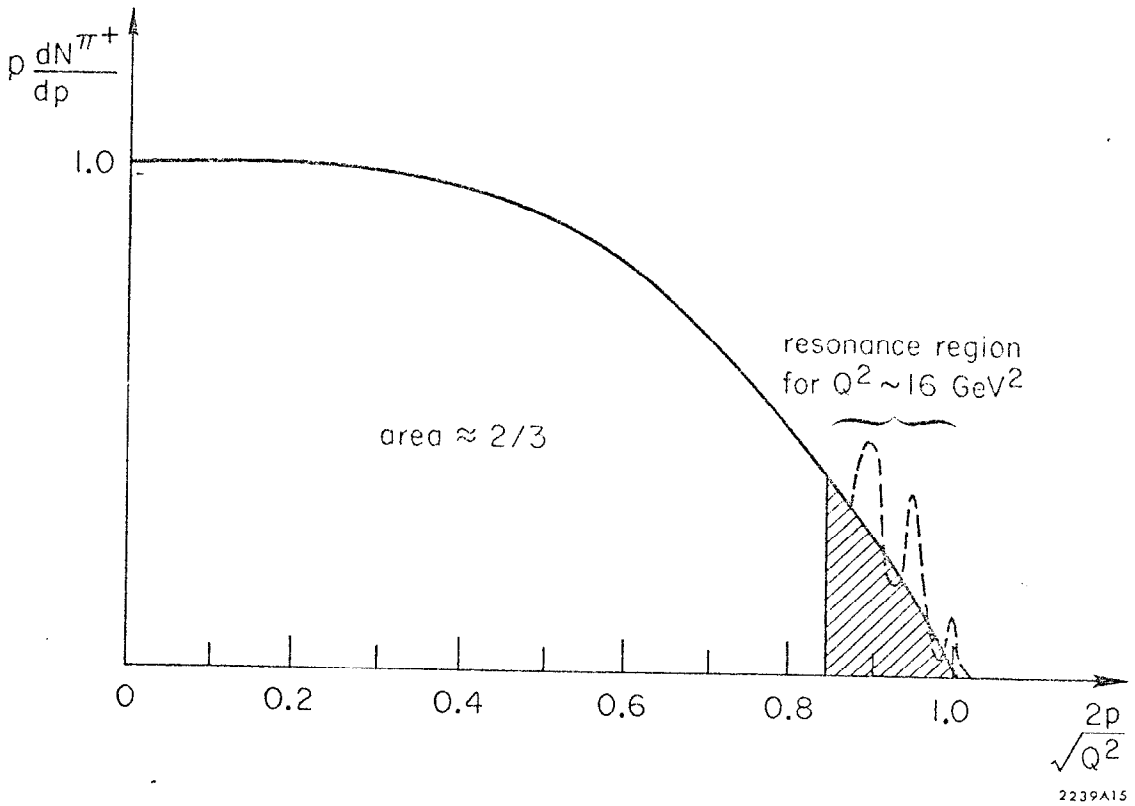
p dN^π+/dp
1.0
resonance region
for Q^2 ~ 16 GeV^2
area ≈ 2/3
0
0.2
0.4
0.6
0.8
1.0
2p/√Q^2
2239A15

Fig. 15

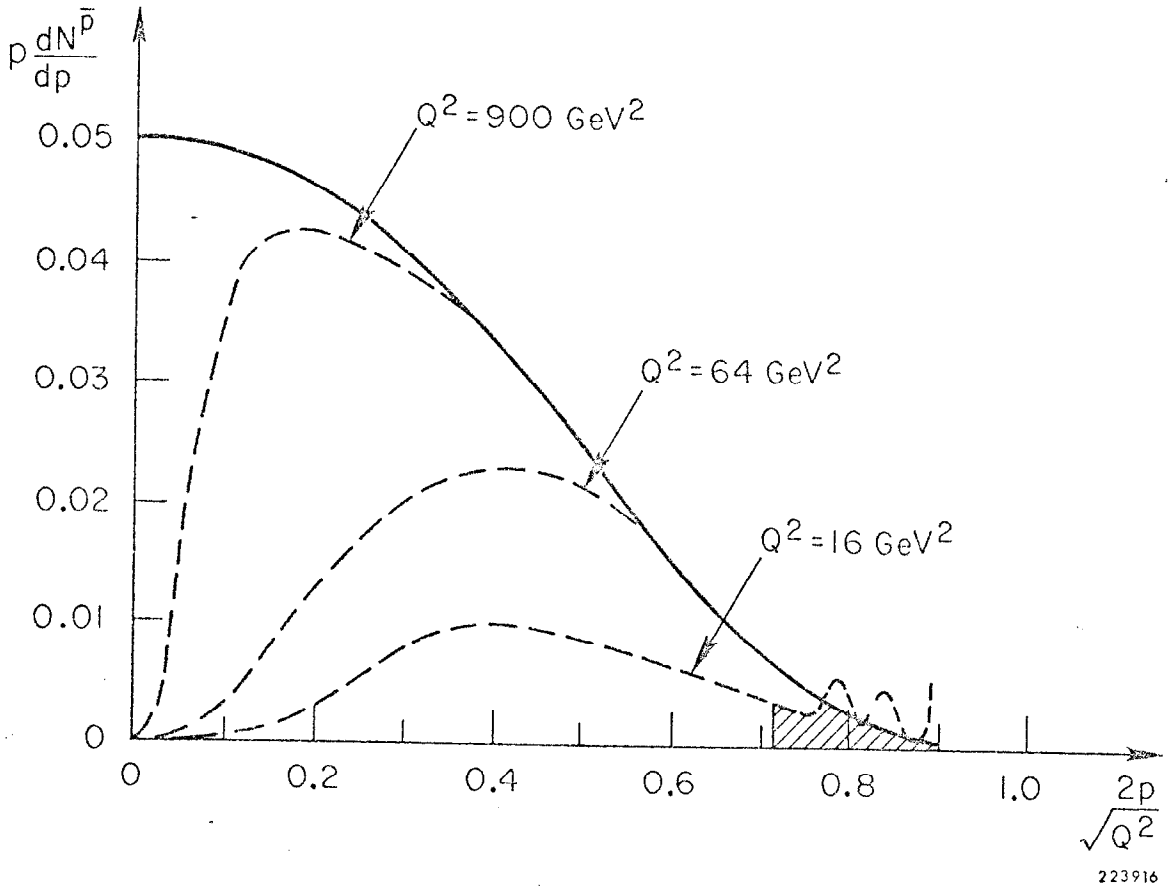
$p\frac{dN^{\bar{p}}}{dp}$
0.05
0.04
0.03
0.02
0.01
0
$Q^2 = 900\ GeV^2$
$Q^2 = 64\ GeV^2$
$Q^2 = 16\ GeV^2$
0
0.2
0.4
0.6
0.8
1.0
$\frac{2p}{\sqrt{Q^2}}$
223916

Fig. 16

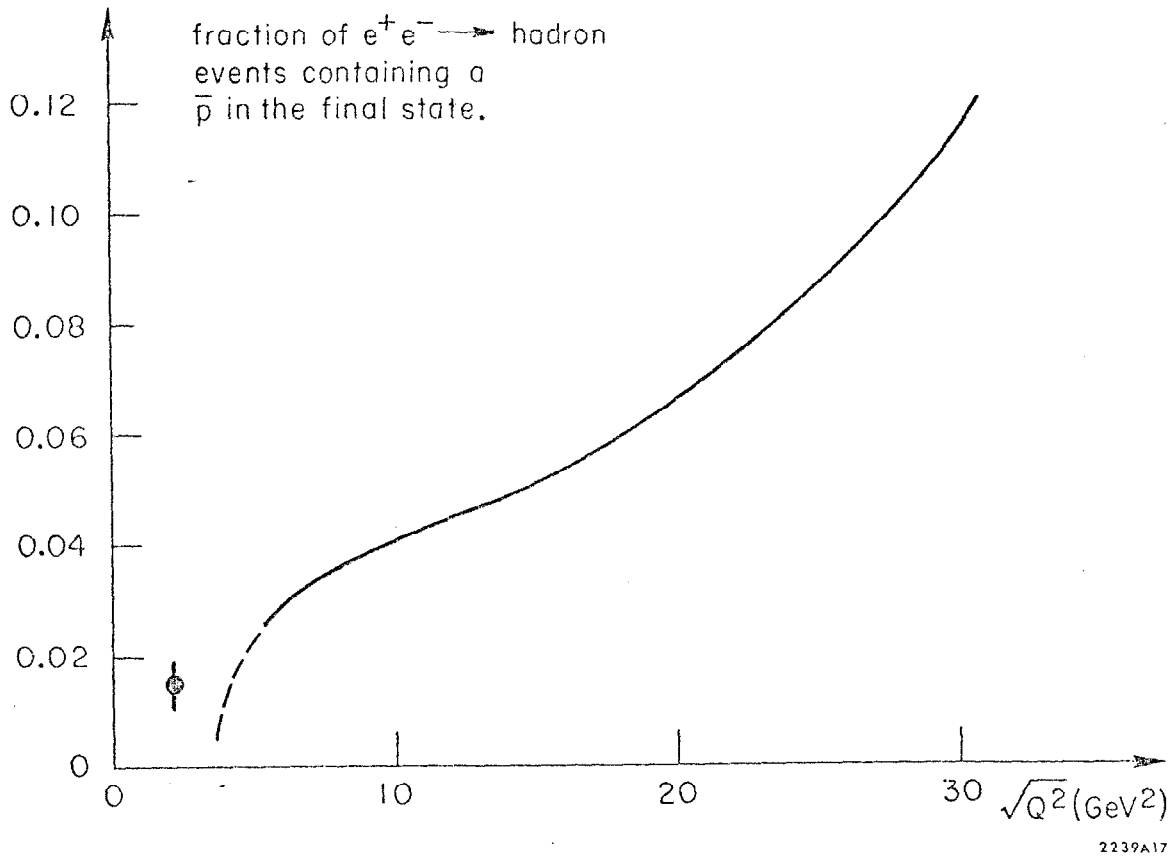
fraction of $e^+e^- \rightarrow$ hadron events containing a $\bar{p}$ in the final state.
0.12
0.10
0.08
0.06
0.04
0.02
0
0
10
20
30
$\sqrt{Q^2}$(GeV)
2239A17

Fig. 17

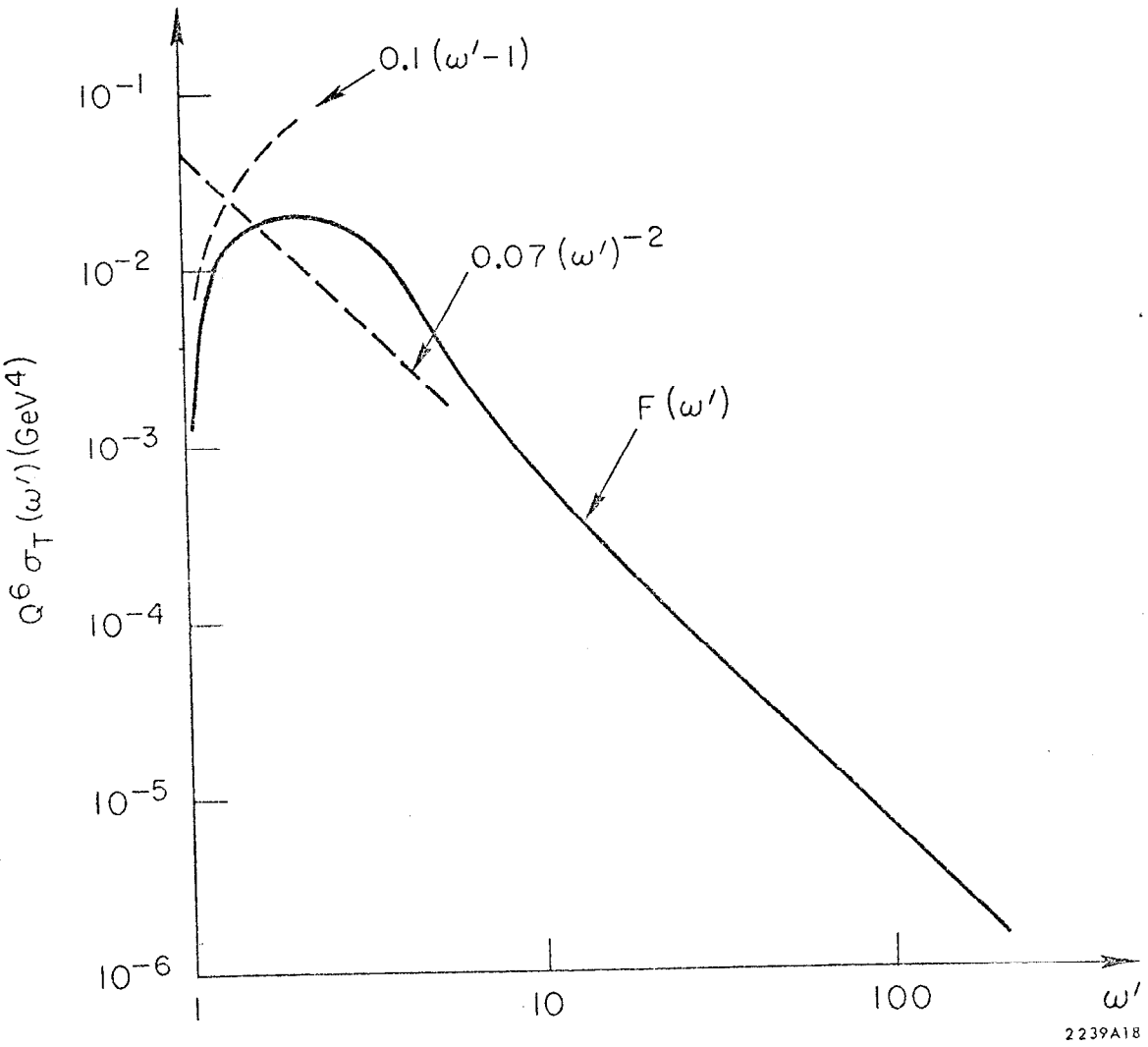
0.1 (ω′−1)
0.07 (ω′)^−2
F (ω′)
10^−1
10^−2
10^−3
10^−4
10^−5
10^−6
Q^6 σ_T (ω′) (GeV^4)
1
10
100
ω′
2239A18

Fig. 18

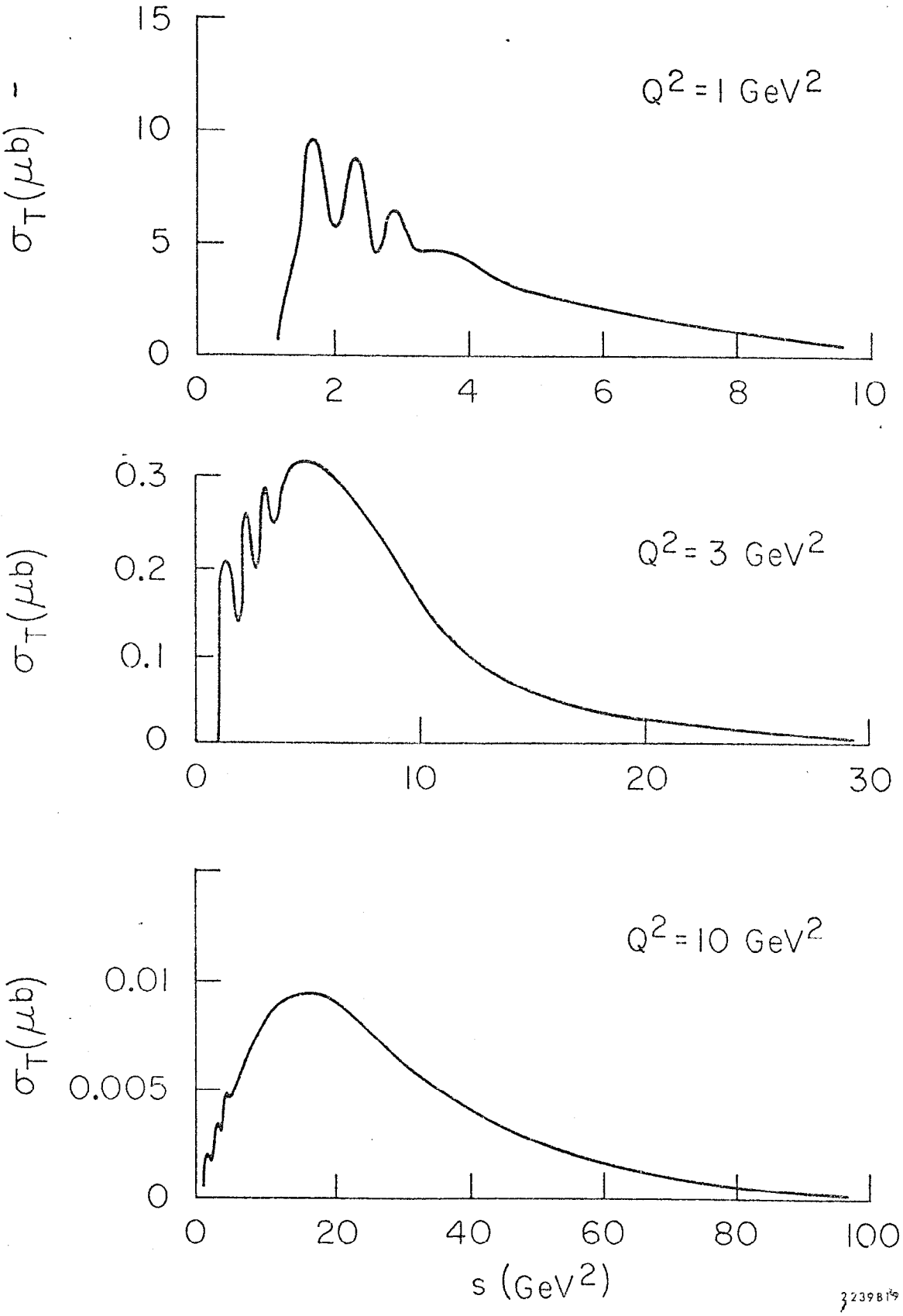
15
10
5
0
$\sigma_T(\mu b)$
$Q^2 = 1\ GeV^2$
0
2
4
6
8
10
0.3
0.2
0.1
0
$\sigma_T(\mu b)$
$Q^2 = 3\ GeV^2$
0
10
20
30
0.01
0.005
0
$\sigma_T(\mu b)$
$Q^2 = 10\ GeV^2$
0
20
40
60
80
100
s (GeV^2)
3239B19

Fig. 19